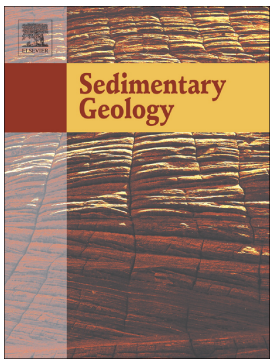

High-resolution compositional analysis of a fluvial-fan succession: The Miocene infill of the Cacheuta Basin (central Argentinian foreland)

Gabriel Hunger, Dario Ventra, Andrea Moscariello, Gonzalo Veiga, Massimo Chiaradia

PII: S0037-0738(17)30271-3
DOI: doi:10.1016/j.sedgeo.2017.12.004
Reference: SEDGEO 5276

To appear in:

Received date: 7 June 2017
Revised date: 29 November 2017
Accepted date: 3 December 2017

Please cite this article as: Gabriel Hunger, Dario Ventra, Andrea Moscariello, Gonzalo Veiga, Massimo Chiaradia , High-resolution compositional analysis of a fluvial-fan succession: The Miocene infill of the Cacheuta Basin (central Argentinian foreland). The address for the corresponding author was captured as affiliation for all authors. Please check if appropriate. Sedgeo(2017), doi:10.1016/j.sedgeo.2017.12.004

High-resolution compositional analysis of a fluvial-fan succession: the Miocene infill of the Cacheuta Basin (central Argentinian foreland)

Gabriel Hunger [a]* Dario Ventra [a], Andrea Moscariello [a], Gonzalo Veiga[b], Massimo Chiaradia [a]

[a] Department of Earth Sciences, University of Geneva, 13 rue des Maraichers, 1205 Geneva, Switzerland

[b] Centro de Investigaciones Geológicas (CIG), Universidad Nacional de La Plata- CONICET, Calle Diagonal 113 N8 275, B1904DPK La Plata, Argentina

*Corresponding author

E-mail address: gabriel.hunger@unige.ch

Abstract

The Miocene infill of the Cacheuta Basin (central Argentinian foreland) comprises the Mariño and La Pilona formations, which record continental sedimentation related to the major phases of uplift of the Andean chain around 33° S over 1500 m of stratigraphy. Sedimentological and stratigraphic evidence suggest the succession to represent progradation of a fluvial-fan sourced from the western, orogenic margin of the foreland basin. The integration of compositional data and sedimentological observations consent to disentangle the relative roles of allogenic factors over long time scales, and to separate them from system-scale autogenic dynamics. The geochemical, mineralogical and radiogenic-isotope composition of sandstones through the succession show a progressive change in

the composition of magmatic source rocks from more primitive (basaltic-andesitic) to relatively more evolved (dacitic), testifying the uplift of the western part of the Principal Cordillera, followed by the sequential eastward advance of the thrust and volcanic fronts towards the foreland basin, in agreement with established chronologies of Andean structural development at these latitudes. Sandstones from the La Pilona Formation record compositional signatures suggesting the first stages of uplift of the Frontal Cordillera. The gradual changes in the compositional signal are attributed to changing weathering conditions related to climate and to source-rock changes, related to the Miocene tectonic evolution of the Andean range. However, results suggest that the influence of large-scale allogenic factors is partly blurred by the effects of autogenic fluctuating depositional processes, especially during deposition of the La Pilona Formation. The gradual transitions in provenance and weathering signals suggest that vertical architectural and facies changes through the succession are likely related to the long-term, progradational evolution of the fluvial-system, rather than to allogenic changes in basin accommodation or climate-related sediment supply.

Keywords: geochemistry, provenance, foreland, fluvial fan, distributive fluvial system, autogenic

1. Introduction

Foreland basins are orogen-related depressions resulting from lithospheric flexure in response to tectonic and sediment loading in collisional settings (Price, 1973; Jordan, 1981; Covey, 1986; DeCelles and Giles, 1996; DeCelles, 2012). Owing to the combination of high sediment supply and prolonged, elevated rates of subsidence, such basins are accurate recorders of processes and environmental conditions during times of orogenic uplift (Dickinson, 1985; Jordan, 1995; Ballato and Strecker, 2014). Many studies have stressed the importance of developing conceptual models that relate vertical and lateral compositional signatures of basin infills to allogenic forcing and autogenic processes (von

Eynatten et al., 2012a, and references therein). In combination with source-area lithology, these factors are responsible for the compositional characteristics of the sedimentary record (Ballato and Strecker, 2014). Many studies have been carried out at the scale of entire formations, based on the identification of compositional changes taking place at major stratigraphic unconformities. However, uncertainties remain in deciphering and interpreting compositional changes at higher resolution and in differentiating the effects of allogenic factors from those related to autogenic dynamics on the basis of compositional signatures (Amorosi and Zuffa, 2011). In continental settings, allogenic factors refer to the influence that climate and tectonics might have on sandstone compositional signatures at regional-scale (Miall, 2014, and references therein), as opposed to autogenic processes, which are internally generated by the depositional system itself and act on a local scale (Amorosi and Zuffa, 2011; Ventra and Nichols, 2014), and which might obscure the possible record of allogenic factors as well as complicate trends in compositional signatures. It is difficult to present a general approach regarding compositional analysis because each sedimentary basin and associated source area have their own characteristics and the possible interactions between different forcing factors may vary greatly. In order to gain information on long-term processes, such as climate and regional tectonics (Dickinson, 1985; Bhatia and Crook, 1986; Etemad-Saeed et al., 2011; Zhang et al., 2013; Ballato and Strecker, 2014; Schlunegger and Norton, 2015), the possible role played by autogenic dynamics also needs to be assessed when interpreting changes in sediment composition through the stratigraphic column (Pearce et al., 1999; Allen and Fielding, 2007; Amorosi and Zuffa, 2011).

The objective of this contribution is to study changes in sediment composition through the early stratigraphic record of continental deposition in the Cacheuta Foreland Basin (west-central Argentina). The temporal evolution of the basin infill is closely related to processes acting during the main phases of Andean uplift during the Miocene (Kay et al., 2005; Charrier et al., 2014). This research focuses on the development of the Mariño and La Pilona formations, regionally and chronologically constrained by Yrigoyen (1993), Irigoyen et al. (2000) and Buelow et al. (2014) as recording the uplift of the Principal and Frontal Cordilleras of the Andes from prior to 18 to 9 Ma. The

study area is located in the eastern slope of the Andes in central Argentina (33° S; Fig. 1), where outcrops of vast extension provide an excellent opportunity to reconstruct the temporal and spatial evolution of processes in proximity to the active Andean orogen. The composite stratigraphic column discussed here is approximately 1500 m thick and comprises sedimentological evidence for the long-term development of a fluvial fan during a period of general climatic aridity. Evidence from different kinds of continental basins and climatic zones worldwide (e.g. DeCelles and Cavazza, 1999; Hartley et al., 2010; Fordham et al., 2010; Weissmann et al., 2010, 2011; Rossetti et al., 2012; Fontana et al., 2014) demonstrates that fluvial fans (also known as distributive fluvial systems; Weissmann et al., 2010; Hartley et al., 2010) are responsible for the aggradation of the largest fraction of sediments in continental basins. These systems show a strong propensity to maintain net aggradation over long timescales (up to 10^{6-7} y) in the presence of continuous subsidence and a positive accommodation balance, and their deposits may thus offer virtually continuous records of surface processes and environmental change. Compositional analysis has been shown to be very useful in elucidating original detrital signatures and the main characteristics of sedimentary rocks (e.g. Long et al., 2008). We present here a high-resolution multiproxy compositional study of the geochemistry (major and trace elements), mineralogy and radiogenic isotope ratios ($^{87}Sr/^{86}Sr$ and $^{143}Nd/^{144}Nd$) of the basin infill, aiming to unveil the relative importance of different, concomitant forcing factors within a known tectonic framework and in the context of development of a fluvial-fan system. A detailed sedimentological and architectural description of the studied succession is beyond the scope of this article, and will be presented in a companion paper (Ventra et al., in preparation).

2. Geological setting

2.1. Regional tectonic history

The Andean Cordillera is an orogenic belt extending along the western, active continental margin of South America, and formed in the context of subduction of the Nazca Plate underneath the South

American Plate (Dewey and Bird, 1970; Gutscher, 2002). Along its strike, the orogen shows a complex variability in its tectonic structure, and broad variations in topography, morphology and volcanism (Jordan et al., 1983a,b; Alarcon and Pinto, 2015; Porras et al., 2016, and references therein) are closely related to the geometric configuration of subduction (Reynolds et al., 1990; Charrier et al., 2007; Ramos, 2009; Dávila et al., 2010; Alarcon and Pinto, 2015; Álvarez et al., 2016; Giambiagi et al., 2016).

The subducted slab of the Nazca Plate is segmented into different sectors from north to south along the Andean Range, based on the variable angle of subduction underneath the overriding continental plate (Reynolds et al., 1990). Two major zones of so-called "flat subduction" (i.e., low angle of subduction dip) are recognized in Peru (approximately between 2° and 15° S) and in western Argentina and central Chile (between 27° and 33° S; Porras et al., 2016), the latter being recognized as the Pampean flat-slab domain of the Central Andes (Gutscher et al., 2000; Ramos et al., 2002; Manea et al., 2012; Álvarez et al., 2016). At 33° S, the Andes of western Argentina and central Chile lie within the zone of transition from flat subduction to the north to higher-angle subduction to the south (Álvarez et al., 2016). At this latitude the Andean Range is characterized by four major morphotectonic provinces established during the Cenozoic, comprising from west to east the Coastal, the Principal and Frontal Cordilleras, and the Precordillera (Fig. 1A). The chronology of development of these provinces has long been a source of debate (Alarcon and Pinto, 2015), but it is well established that deformation and uplift started in the western sector of the orogen in the Early Miocene (Ramos, 1996a), advancing progressively toward the continent during the Neogene and Quaternary, with eastward migration of arc-related magmatism and sequential uplift of the different morphotectonic units (Ramos et al., 2002; Giambiagi and Ramos, 2003; Fock Kunstmann, 2005; Charrier et al., 2014; Giambiagi et al., 2016).

The compressional phase in the region started in the Early Miocene, during uplift of the Coastal and Principal cordilleras (Giambiagi et al., 2016), with tectonic inversion of the Mesozoic and early

Cenozoic former extensional Abanico Basin in the western sector of the Principal Cordillera (Giambiagi and Ramos, 2003). Magmatic activity was concentrated in this sector, with the emplacement of volcanic rocks and volcaniclastic deposits of the arc-related Farellones Formation overlying the Oligocene-Miocene Abanico Formation (Fock Kunstmann, 2005). Eastward migration of the deformation front started around 18 Ma (Giambiagi et al., 2001; Giambiagi and Ramos, 2003; Kay et al., 2005; Giambiagi et al., 2009), concentrating in the eastern Principal Cordillera and involving Mesozoic sedimentary successions into the Aconcagua Fold and Thrust Belt (AFTB; Cegarra and Ramos, 1996; Cristallini and Ramos, 2000). Around this time, foreland subsidence started recording Andean uplift at these latitudes in the Alto Tunuyán Basin (34° S), with the proximal Tunuyán Conglomerates overlying the volcanic Contreras Formation (dated at 18.3 Ma; Giambiagi and Ramos, 2002), and recording more distal foreland sedimentation in the Cacheuta Basin (33°S) with the coeval Mariño Formation overlying the Divisadero Largo Formation (Giambiagi and Ramos, 2003).

High rates of crustal shortening in the Middle Miocene were accompanied by increasing accommodation in the central Andean foreland (Irigoyen et al., 2000; Perez, 2001; Giambiagi et al., 2016). Bedrock sources for foreland synorogenic strata were restricted to uplifted volcanic and sedimentary rocks of the western and eastern Principal Cordillera (Giambiagi et al., 2014). The Teniente Plutonic Complex at 34° S (14.4 – 7 Ma) started intruding the Abanico and Farellones formations (Kay et al., 2005) in the western Principal Cordillera, and the first migration of the volcanic front towards the east is represented by the Aconcagua Volcanic Complex (15.8 – 8.6 Ma; Ramos et al., 1996b; Charrier et al., 2014).

In the Late Miocene the proximal Alto Tunuyán Basin was affected by out-of-sequence thrusting and creation of a major stratigraphic unconformity, defining the beginning of deposition for the Palomares Formation (Giambiagi and Ramos, 2003). In the more distal Cacheuta Basin this unconformity, which is probably related to peak rates of uplift at ca. 12.5 – 10 Ma (Alarcon and Pinto, 2015), is geometrically less pronounced, showing a very low angle (2 – 4^{o}) to the local stratal

geometry, and marks the transition from the Mariño Formation to the La Pilona Formation (Irigoyen et al., 2000; Giambiagi and Ramos, 2003). The eastward advance of the deformation front, triggering the uplift of the Frontal Cordillera, starts to be recorded in both basins around 12 – 10 Ma (Irigoyen et al. 2000; Giambiagi et al., 2001). Uplift of the Frontal Cordillera was expressed diachronously farther north by the topographic ranges of the Cordon del Tigre (32°S) and successively by the Cordon del Plata at 33°S around 10 Ma (Giambiagi and Ramos, 2003). The topographic expression of the Frontal Cordillera is presently limited to the northern part of the normal subduction segment, disappearing toward the south at approximately 34°S (Giambiagi et al., 2016). The Frontal Cordillera was uplifted during the eastward advance of the deformation front by east-verging thrust faults (Porras et al., 2016) connected to a décollement level in Jurassic evaporites (Fock Kunstmann, 2005). The foreland basin was then broken apart (*sensu* Jordan, 1995; Strecker et al., 2012) during the uplift of basement blocks which exposed Proterozoic metamorphic rocks (Porras et al., 2016), late Palaeozoic marine successions (Polanski, 1958; Gutiérrez et al., 2006) and intrusive rocks (Polanski, 1964) and Early Triassic volcanic rocks of the Choiyoi Group (Kleiman and Japas, 2009). Initial uplift of the Precordillera took place with further eastward migration of the flat-slab system and has been constrained at ~10 Ma (Walcek and Hoke, 2012), coeval with the continued uplifting of the Frontal Cordillera. The latter prevented the propagation of the thrust belt towards the Cacheuta foreland basin (Giambiagi et al., 2016), whose exposed stratigraphic successions remain to date only gently folded and affected by minor faulting in the study area.

2.2. Stratigraphic and sedimentological framework

Previous studies link the sedimentary infill of the Cacheuta Basin to the first stages of development of the main Andean range (Irigoyen, 1997; Irigoyen et al., 2000; Giambiagi and Ramos, 2003; Giambiagi et al., 2014; Giambiagi et al., 2016). The onset of foreland sedimentation is coeval with a major phase of thrusting in the AFTB (Ramos et al., 1996a; Cegarra and Ramos, 1996; Irigoyen et al., 2000). The studied succession is ~1500 m thick and comprises the Mariño Formation and the La

Pilona Formation. According to magnetostratigraphic and geochronometric data by Irigoyen et al. (2000), the Mariño Formation was deposited approximately between 15.7 and 12.03 Ma. However, Buelow et al. (2014) recently dated the onset of foreland deposition as antecedent to 18 Ma, in agreement with mammal fossil ages obtained by Cerdeño and Vucetich (2007), and suggesting a revision of previous magnetostratigraphic age constraints (Giambiagi et al., 2016).

The Mariño Formation conformably overlies the Divisadero Largo Formation, which is composed of fine-grained clastics, gypsum and anhydrite horizons, interpreted as an ancient continental sabkha to mudflat system (Kokogian and Mancilla, 1989; Irigoyen et al., 2000) established before the onset of the major phase of foreland-basin subsidence (Sempere et al., 1994). The basal, alluvial member of the Mariño Formation (Irigoyen et al., 2000; ca. 100 m in thickness; Fig. 2A) consists of dominantly muddy, weakly to moderately pedogenised alluvium with isolated, sandy to fine gravelly, ribbon-shaped channel bodies, representing deposition on a distal, low-gradient alluvial plain. Isolated channel fills (*sensu* Owen et al., 2017) comprise mostly multistorey and rarely single storey elements composed of moderately to poorly sorted, fine- to coarse-grained sandstones and gravelly sandstones organized in fining-upward facies successions. The largest volume of coarse sediment in channel bodies is represented by three facies: i) low-angle cross-stratified sandstones and fine-gravelly sandstones in centimetric to decimetric sets of downstream- and less commonly upstream-dipping laminae; ii) massive to crudely plane-stratified, poorly to moderately sorted sandstones and gravelly sandstones, featuring coarse-tail normal grading and crude imbrication of pebble-grade clasts; iii) massive to crudely plane-stratified pebble conglomerates with poorly sorted sandy matrix. These facies reflect mostly rapid deposition of relatively coarse bedload from sediment-charged, transcritical to supercritical currents (e.g. Long, 2002; Fielding, 2006; Cartigny et al. 2014; Lowe and Arnott, 2016) and rapid to gradual aggradation from high-concentration sediment dispersions in which clasts were supported by buoyancy and hindered settling, unable to sustain bedform migration at the depositional interface (e.g. Smith, 1986; Billi, 2008; Long, 2017). Mudstone facies are dominant in this interval and comprise massive to thinly bedded, poorly lithified claystones and minor

siltstones with scarce evidence for pedogenic modification, except for rare interbedded horizons of carbonate concretions. The overall evidence points to deposition from unconfined, shallow flows over a distal floodbasin (Bridge, 2003; Cain and Mountney, 2009) where continuous aggradation prevented the establishment of mature palaeosols. However, mudstones feature rhythmic patterns in colour and mottling density which probably relate to climatic and hydrological changes affecting sediment supply and incipient pedogenesis (Kraus and Hasiotis, 2006; Abels et al., 2013; Fig. 2A). The overlying member of the Mariño Formation, 180 to 200 m thick, consists mostly of well-sorted, cross-stratified sandstones in sets of thickness variable from a few decimetres to ~15 – 18 m, comprising grainfall and grainflow laminae (Kocurek and Dott, 1981) and representing accumulation from dunefields developed in a persistently dry aeolian system (Wilson, 1973; Kocurek and Havholm, 1993; Fig. 2B), thus indicating the prolonged establishment of an erg landscape. In the topmost few tens of metres of this intermediate member, isolated associations of thinly bedded mudstones, clayey fine sandstones and marlstones represent deposition from suspension settling, traction from low-energy currents and biogenic accumulation in wet interdunes (e.g. Lancaster and Teller, 1988; Fryberger, 1990). Combined with large lenses of alluvial deposits (up to a few tens of metres thick, many hundreds of metres wide), these elements suggest occasional persistence of the water table in proximity of the surface and local breaching of the erg margin by runoff (Stanistreet and Stollhofen, 2002; Liu and Coulthard, 2015). This indicates possible interactions with an already active fluvial system and/or possible return to relatively humid conditions.

The establishment of the erg system might have been induced by climate aridification and /or by a regional repositioning of the main fluvial system. Aridity would have promoted sand availability and the transport capacity of winds, making aeolian accumulation locally more important than alluvial deposition (Tripaldi and Limarino, 2005), further creating a complex topography that would have induced drainage repositioning on a regional scale. Similar, roughly coeval aeolian successions have been identified across the Andean foreland and elsewhere in central South America (Milana et al., 1993; Perez, 2001; Tripaldi and Limarino, 2005), reflecting a common response across different

basins to probable climatic forcing during the early foreland history**.** The great thickness of the aeolian members in the Vallecito Formation (29°30' S, Tripaldi and Limarino, 2005), Chinches Formation (32° S, Perez, 2001), Pachaco Formation (31°30' S, Milana et al., 1993), as well as in the Mariño Formation described here (Irigoyen, 1997; Irigoyen et al., 2000), reflects a probable combination of enhanced early subsidence (Tripaldi and Limarino, 2005), favouring topographic preservation of aeolian deposits (Wilson, 1971; Kocurek and Havholm, 1993), and increased deflation and redeposition of unconsolidated sediments within the foreland.

The overlying 800 m of stratigraphy belong to the topmost, thickest member of the Mariño Formation, dominantly alluvial in origin, consisting of vertically alternating, amalgamated channel fills and mudstone-dominated overbank deposits (Fig. 2C). Channel fills form laterally extensive, sheet-like bodies (internally amalgamated channel sheets of Owen et al., 2017) comprising the same sandstone and fine conglomerate facies described above for the lower alluvial member of the Mariño Formation, deposited from supercritical and highly concentrated flood flows. Channel bodies commonly lack the hierachical stratal architecture indicative for development of complex macroforms (Crowley, 1983; Miall, 1985) and present a simple vertical stacking of depositional units. Facies associations and architectures are thus typical for rapid, ephemeral episodes of aggradation in channels subject to flash-flood events triggered by sporadic, intense rainfall (Hassan, 2005; Laronne & Shlomi, 2007; Powell, 2009), and suggest a persistent arid to semiarid climate also during accumulation of this topmost alluvial member of the Mariño Formation (Irigoyen, 1997; Franco et al., 2014). This inference is confirmed by the scarcity of pedogenic signatures and by the bright red colours of mudstone units, suggesting the poor soil development under strongly oxidizing conditions typical of arid subaerial environments hosting permanently well-drained floodplains (Dill, 1995; Kraus and Riggins, 2007).

The La Pilona Formation overlies the Mariño Formation (Yrigoyen, 1993) through a low-angle stratigraphic unconformity and records foreland deposition approximately from 11.7 Ma to 9 Ma

(Irigoyen et al., 2002). It consists mostly of amalgamated fluvial-channel fills (massive to semi-amalgamated channel bodies of Owen et al., 2017) and with negligible volumes of preserved overbank mudstones (Fig. 2D). Sedimentary facies in channel bodies are represented by dominant conglomerates and gravelly sandstones, mostly comprising massive to plane-stratified deposits from bedload sheets and hyperconcentrated flows (Whiting et al., 1988; Todd, 1996), and only local occurrence of cross-stratified sandstones and conglomerates representing occasional development (and/or low preservation potential) of subaqueous dunes and low-relief bars under conditions of lower flow regime (Crowley, 1983; Todd, 1996). Facies associations are thus still typical for flash-flood deposition under mostly ephemeral discharge conditions, indicating a substantial palaeohydrologic analogy with ephemeral-flood deposits of the underlying Mariño Formation.

For the entire succession, vertical facies and architectural trends are consistently traceable laterally throughout the system's outcrop extent, without significant variations, and are thus representative for the progressive development of an extensive fluvial system in the region, only temporarily interrupted by the establishment of an aeolian dunefield. The sampled interval (see following section 3.1) spans the sedimentary succession described above, which shows a progressive upward increase, through stratigraphy, in grain sizes of alluvial channel fills, and especially in the dimensions and relative volume of amalgamated channel fills, with a concomitant decrease in the relative volume of preserved overbank fines. The continuity in sedimentation throughout the system's history is supported also by the invariance of palaeocurrent trends, which consistently vary from southeast to northeast, indicating basinward transport of debris shed from the Andean orogen. These architectural and facies trends are in agreement with conceptual models of vertical stratigraphic architecture related to long-term aggradation and progradation of fluvial fans (or "distributive fluvial systems"; Nichols and Fisher, 2007; Weissmann et al., 2010, 2013; Owen et al., 2015). This is also confirmed by the dominantly aggradational architecture of the succession through many hundreds of metres in stratigraphy and over many kilometres along outcrop strike, lacking any evidence for deep channel incision, valley confinement or terracing. The large-scale architecture of alluvial strata is

dominated by laterally continuous, essentially tabular clastic packages with minimal erosion, related to the dominantly avulsive dynamics of channel belts (e.g. Stear, 1983; Rust and Gibling, 1990; Gibling, 2006). The inferred progradation of a long-lived fluvial-fan system sourced from the western orogenic margin of the basin is supported also by geomorphic evidence for modern distributive fluvial systems dominating vast alluvial tracts in direct proximity of presently active orogens (Gupta, 1997; Hartley et al., 2010; Weissmann et al., 2013), and by case studies recognizing similar systems to have dominated alluvial aggradation in ancient foreland basins (e.g. Schlunegger et al., 1997; DeCelles and Cavazza, 1999; Uba et al., 2006; Fontana et al., 2014; Owen et al., 2015).

3. Methods

3.1. Sampling strategy

The studied stratigraphic interval consists of an approximately 1500 m-thick composite log, comprising the entire Mariño Formation and the basal hundreds of metres of the La Pilona Formation, cropping out along the exposed limbs of the La Pilona Anticline along the National Road 7 connecting Mendoza to Santiago de Chile (Fig. 1B), ~11 km south of the village Potrerillos. The studied section consists of a composite of different logs (varying in thickness from a few tens to several hundreds of metres) measured at different locations across the outcrop belt (Figs. 1B and 2), depending on accessibility and quality of preservation; correlations between logs were obtained by walking out recognizable stratal surfaces and/or extensive mudstone units. A total of 83 sandstone samples were collected from this composite stratigraphic section (Figs. 1B and 2), attaining the average resolution of one sample every ~17.5 m of the sedimentary column. Each main sandstone unit within the Mariño and La Pilona formations was sampled, representing laterally continuous, amalgamated channel-belt deposits as well as associated strata of aeolian origin. Samples were collected from relatively unweathered portions of outcrops, in order to avoid the effects of recent weathering on the original composition. In order to reduce grain-size biasing of whole-rock composition, field sampling was restricted to fine- to medium-grained sandstones. Possible biasing

effects due to variable depositional mechanics were avoided by restricting the sampling to facies originated from supercritical and high-concentration currents, which represent by far the majority of channel fills (see previous section) and accumulated from rapid sediment dumping, with minimal reworking and clast segregation by size and/or density. Clay-rich and gravelly sandstones were not sampled in order to avoid deviations in compositional signatures related to enrichment in clay-minerals and/or to the presence of large clasts. The complete database of geochemical, mineralogical and isotopic results is available online in Excel file format as supplementary data (Appendix 1).

3.2. Whole-rock geochemistry (XRF)

Whole-rock geochemical analyses of sandstone samples were performed at the laboratories of the Department of Earth Sciences, University of Geneva, and at the Faculty of Geosciences and Environment, University of Lausanne. Samples were dried at 110°C in a heat chamber to remove any residual humidity and then crushed into powder with an automated mortar grinder. They were then analysed by X-ray fluorescence spectrometry (XRFs) using a PANalytical Axios™ spectrometer.

For quantifying major elements, 3 g of crushed powder were preliminarily heated for three hours in an oven at 1150°C, in order to eliminate volatile components (loss on ignition; LOI). Subsequently, 6 g of lithium tetraborate were added to 1.2 g of the calcinated product and pounded with a glass mortar for homogenization. The resulting powder was poured in a platinum crucible and processed in an automated glass-bead-casting machine (Eagon2™) in order to obtain a glass disc to be analysed. For quantification of trace elements, 3 g of wax were added to 12 g of crushed sample. To prepare a pressed disc, a 10 ton load was applied on the homogenised mixture for 20 seconds with a hydraulic press.

The analytical standards used are BHVO, NIM-N, NIM-G, SY2, JCH-A and UB-N for the silicate fraction, and TS2 and ST 393 for samples enriched in calcite (Govindaraju, 1994). The results for major elements are reported in weighted percentages corrected for LOI, with an accuracy of approximately

0.4%, and in parts per million (ppm) for trace elements, with an accuracy of 1 to 3 ppm and a maximum of 7 ppm (for lanthanum).

3.3. Automated petrography (QEMSCAN®)

Automated petrographic analyses were performed at the QEMSCAN® laboratory of the University of Geneva on polished and carbon-coated thin sections and plugs from the same sandstone samples subjected to XRF analysis. Analyses were carried out under high vacuum conditions (10^{-6} mbar) and at an acceleration voltage of 15 kV with a probe current of 10nA. The acquisition time of the energy-dispersive X-ray signal (EDS) was approximately 200 pixels per second using a point-spacing of 5 µm. Mineral-phase identification was automatically performed by comparing EDS spectra of individual pixels with a database of standard spectra provided by the manufacturer (FEI Company).
Data were processed with the FEI iDiscover™ software; manual debugging of measurements included the identification of mixed signals on grain boundaries, unidentified labeled pixels, and inaccurate mineral determinations. In order to obtain an acceptable final result including less than 5 % of unidentified pixels, EDS spectra and elemental concentrations were compared with available databases. Spurious mineral signatures were constrained using conventional microscopic petrography on thin-sections. The precise identification of clay minerals was performed by comparing QEMSCAN® results with XRD measurements performed at the University of Geneva. The database was then fine-tuned by subsequent observations. For each sample, a scan image was produced showing all identified minerals. The abundance of each mineral was finally estimated by quantifying its occurrence as surface percentages.

3.4. Strontium and neodymium isotopes

For this study, whole-rock Sr and Nd isotopic compositions of siliciclastic sediments were used to help infer the average igneous affinity of the source lithotypes (Faure, 2001). Radiogenic isotope

analyses were performed at the Department of Earth Sciences of the University of Geneva on a Neptune Plus® MC-ICPMS using Faraday cups. The methodology, standards used and error evaluations are extensively described in Chiaradia et al. (2011) and Béguelin et al. (2015). The reproducibility of the Nd and Sr analyses based on long-term measurements (N>100) of the JNdi-1 ($^{143}Nd/^{144}Nd$ = 0.512115; Tanaka et al., 2000) and SRM 987 ($^{87}Sr/^{86}Sr$ = 0.710248; McArthur et al., 2001) is <20 ppm (2s). Whole-rock isotopic ratios of $^{87}Sr/^{86}Sr$ and $^{143}Nd/^{144}Nd$ were measured on 17 sandstone samples selected for best representation of the range of composition along the stratigraphic column. In order to facilitate the interpretation of measured $^{143}Nd/^{144}Nd$, the epsilon notation (ε_{Nd}) was used (DePaolo and Wasserburg, 1976a,b; Faure, 2001). The epsilon parameter compares the measured $^{143}Nd/^{144}Nd$ ratio of a rock sample to the $^{143}Nd/^{144}Nd$ ratio of the Chondritic Uniform Reservoir (CHUR = 0.512638; Wasserburg et al., 1981; Saitoh et al., 2011).

3.5. Statistics

In order to interpret element associations and mineralogical control on composition, part of the data was examined by means of a principal component analysis (PCA; Bhatia and Crook, 1986). This statistical method combines different variables from a dataset into several independent latent variables that underlie the multivariate data (Ohta and Arai, 2007). The final result is a visual representation of the data into newly created dimensions, called Principal Components, that better represent the compositional variability, highlighting the importance of specific elements and mineral phases in defining the whole-rock compositional variability (Zhang et al., 2013). An advantage of the PCA is that different mineral phases and elemental compositions are grouped by their common behaviour within the dataset, whether they be correlated, uncorrelated or inversely correlated along the stratigraphic succession (Garzanti and Resentini, 2016). In this study the prevailing minerals detected by the QEMSCAN® and the major elements were subjected to PCA calculations. Statistical calculations were performed in the software environment for statistical computing and graphics R

and using "FactoMineR" (Lê et al., 2008) and "compositions" (Van den Boogaart and Tolsana-Delgado, 2008) packages. The centered log-ratio transformation was applied to the data in order to remove constant-sum as well as the non-negativity constraints (Aitchinson, 1982).

4. Results

4.1. Geochemistry and mineralogy

Sandstones from the Mariño and La Pilona formations classify as lithic arenites or argillaceous lithic arenites (*cf.* Dott, 1964), depending on variable clay matrix content (generally less than 15 %), and mostly comprise quartz and feldspathic grains, with variable abundances of volcanic-rock fragments. The sandstones are texturally immature, moderately sorted, with angular to subangular grains of generally low sphericity. Sandstones from the aeolian member of the Mariño Formation are generally well sorted and contain subangular to subrounded grains of low to high sphericity. Based on whole-rock geochemistry by XRF and automated QEMSCAN® petrography (Allen et al., 2012) used to explore the general trends in compositional signature throughout the succession, seven units (letter-coded A to G; Fig. 3) were identified on the basis of major compositional and sedimentological changes.

Samples from the lowermost interval (Unit A) of the Mariño Formation, which comprises dominant alluvial mudstones and isolated, mostly fine-grained channel fills, are enriched in calcite (Fig. 3), and petrographic observations show great amounts of carbonate clasts and pore-filling calcitic cement. In terms of primary sediment composition, Unit A has a very variable pattern, the most relevant attribute being the high concentration of anorthite compared to albite, as observed also in Unit B, which shows an increasing volume of coarser sandy channel fills compared to Unit A. Albite is enriched in samples of aeolian sandstones from erg deposits of Unit C, resulting in the high Na_2O concentration of this unit. Overlying units D to F identified through the Mariño Formation (Fig. 3) present a growing relative volume of increasingly coarse (up to cobble grade in Unit F) and more amalgamated fluvial channel fills, accompanied by decreasing volumes of overbank associations

consisting of mudstone 'redbeds' and sandstone sheets (Fig. 2C). Unit D is characterized by progressive depletion of plagioclase and enrichment in K-feldspar. Except for high peaks in biotite content, the abundances of other major elements and mineral phases are quite variable and do not present any relevant trends.

At a stratigraphic height of 688 m along the logged transect (Fig. 3), at the transition between units D and E, concentrations of albite and Na_2O decrease significantly compared to the underlying intervals. At the same stratigraphic position, the clay mineral kaolinite shows a marked increase in its relative proportion compared to underlying strata, where it was nearly absent, whereas biotite decreases and amphibole increases in abundance. Throughout the stratigraphic column, the trend of K-feldspar abundance is very similar to that of quartz, and is opposite to that of albite.

Only Unit G has been identified within the La Pilona Formation, which consists mostly of medium to coarse sandy to conglomeratic, amalgamated fluvial channel fills with minor volumes of fine overbank deposits. Whole-rock mineralogical data for the La Pilona Formation show different patterns than the Mariño Formation; notably, plagioclase content drops significantly, while quartz and clay-minerals concentration reach their highest levels. Concentrations of Fe_2O_3 and TiO_2 in samples from both formations are positively correlated and are related to the presence of heavy Fe-Ti-bearing minerals (0.5 – 4.25 % of abundance). Other heavy minerals of interest for the La Pilona Formation, detected by the QEMSCAN®, are pyroxenes, which show very low abundance (0.09 – 1.96 %), and amphiboles, which present very variable abundance (from 0.88 to 6.75 %) through the formation.

Trace-element concentrations present more gradual trends (Fig. 4) throughout the stratigraphic succession, with few differences between the identified compositional units. Incompatible elements (Rb, Y, Zr, Nb, La, Nd, Pb, Th) progressively increase, especially from units A and B to the overlying aeolian and fluvial units, whereas compatible elements (Sc, V, Mn, Co, Ni, Cu) display overall decreasing trends through stratigraphy. In the lowermost units A and B, trace-element

concentrations display highly variable values, probably reflecting a strong influence of hydrodynamic sorting due to variable depositional processes, whereas values for sandstones from aeolian facies of Unit C exhibit very low variability. In the overlying fluvial units (D to F) the trace-element curves display several spikes and dips of lower amplitude than in the lowermost fluvial units (A and B) from the Mariño Formation. Despite the lower sampling resolution, compositional variability between samples from Unit G is higher, probably indicating a stronger influence of hydrodynamic sorting in the main compositional signal during deposition of the La Pilona Formation. Stratigraphic trends in the abundance of all major and trace elements are displayed in Appendix 2 as supplementary data online.

4.2. Geochemical proxies for tectonic and climatic settings

For inferences on the general tectonic setting, sample data from the Mariño and La Pilona formations were plotted in the K_2O/Na_2O vs SiO_2 diagram proposed by Roser and Korsch (1986; Fig. 5), commonly used in provenance studies (e.g. Akarish and El-Gohary, 2008; Etemad-Saeed et al., 2011; Alessandretti et al., 2013). Overall, samples plot in the island arc field, and the evolution toward the top of the stratigraphic column shows a trend toward active continental margin, probably related to sediment yield from relatively more evolved magmatic bedrock sources and thus an increase in the compositional maturity of sandstones. However, the applicability of this diagram is strongly dependent on the lithology (Spalletti et al., 2012) as sandstones enriched in clay-minerals are depleted in SiO_2 and enriched in K_2O/Na_2O due to high illite content (Spalletti et al., 2012). Classification problems might also occur with respect to the amount of calcite in the sedimentary rocks. In samples from the Mariño and La Pilona formations, CaO values show strong similarities with relative values of LOI and calcite (Appendix 1). Hence, samples from Unit A, enriched in calcite, are relatively depleted in SiO_2. Sandstones from units D, E and F fall within a transitional domain between the two tectonic settings, whereas sandstones from the La Pilona Formation do not plot within a specific field as they show a wide range of compositional values.

The Th-Sc-Zr/10 ternary diagram proposed by Bhatia and Crook (1986; Fig. 6) is based on the study of immobile trace elements (Th, Sc and Zr) that are not sensitive to remobilization during weathering, diagenesis and metamorphism. The samples from the lower part of the succession plot in the island arc field (Fig. 6). However, samples from stratigraphic intervals overlying the aeolian member show higher concentrations of Th and Zr and plot within the compositional field representative of active continental margins. Overall, the evolution of the compositional signature through the basin infill shows a trend reflecting increasing sediment supply from relatively more evolved magmatic sources.

The bivariant plot of SiO_2 against total Al_2O_3+K_2O+Na_2O proposed by Suttner and Dutta (1986; Fig. 7) has been used for a general inference of climatic conditions during deposition of the Mariño and La Pilona formations. The plot is potentially indicative of chemical maturity trends as a function of climate (Suttner and Dutta, 1986; Hall and Smyth, 2008; Adeigbe and Jimoh, 2013; Zaid et al., 2015), given the lesser mobility of SiO_2 compared to other main-element oxides under the action of surface weathering agents. All samples plot within the aridity domain, in agreement with inferences on depositional processes derived from facies analysis (see above) and with the study of Franco et al. (2014) who recently discussed records of petrified wood from the aeolian member of the Mariño Formation, indicating the presence of aridity-tolerant Late Miocene floras similar to modern Patagonian vegetation.

4.3. Chemical classification of the sandstones

Based on the geochemistry of clastic sedimentary rocks, several authors have proposed chemical classification schemes (Hossain et al., 2014, and references therein). One of the most commonly adopted classifications is the log(Na_2O/K_2O) vs. log(SiO_2/Al_2O_3) diagram proposed by Pettijohn et al. (1972; Fig. 8). The SiO_2/Al_2O_3 ratio provides a chemical differentiation between clay-rich and quartz-rich rocks, hence a first-order discrimination between mudrocks and sandstones (Herron, 1988; Pe-Piper et al., 2008), whereas the Na_2O/K_2O ratio is a measure of plagioclase versus K-feldspar content (Bhatia, 1983; Herron, 1988) and provides potential information about compositional changes

related to weathering conditions, plagioclase being more sensitive to weathering. The samples from the Mariño and La Pilona formations plot mostly in the greywacke field showing a low compositional maturity, consistent with their syntectonic origin in a convergent tectono-magmatic setting (Irigoyen et al., 2000). The sandstones display a progressive trend towards the litharenite field, related to a gradual depletion in plagioclase content and an increase in K-feldspar (also seen in Fig. 3), responsible for decreasing values of $\log(Na_2O/K_2O)$ and slightly increasing values of $\log(SiO_2/Al_2O_3)$, described as an indicator of mineralogical maturity (Pettijohn et al., 1972). The trend seen in figure 8 thus also indicates an increase in sandstone compositional maturity upward through stratigraphy.

4.4. Weathering and maturity

The weathering history of the sandstones can be evaluated using the Chemical Index of Alteration (CIA; Nesbitt and Young, 1982). This tool has proved to be useful in examining compositional variations of mudstones as well as sandstones, due to changes in the intensity of weathering in the source area (e.g., Fedo et al., 1995; Price and Velbel, 2003; Goldberg and Humayun, 2010; Shao and Yang, 2012; Alarcon and Pinto, 2015; Nagarajan et al., 2015; Zaid et al., 2015; Garzanti and Resentini, 2016). This index can be calculated using molecular proportions of major element oxides (Eq. 1):

$$CIA = \left(\frac{Al_2O_3}{Al_2O_3 + K_2O + Na_2O + CaO^*}\right) \times 100 \quad (1)$$

where CaO* represents the calcium in the silicate fraction (McLennan, 1993; Goldberg and Humayun, 2010). In such formulation it is necessary to correct for the presence of Ca in the carbonate fraction, occurring mainly as calcitic cement in the current case, and coming from apatite (corrected using P_2O_5). The QEMSCAN® data was not used for the quantification of calcium content coming from

carbonate and apatite. This automated petrographic tool allows the quantification of sandstone mineralogy from thin-sections, which represent only a fraction of the sandstone sample, the latter not being entirely homogeneous. It is still unclear whether QEMSCAN® technology is reliable for quantification of the geochemistry of sandstone samples. The preferred methodology to calculate CaO* was the one described by Hossain et al. (2014) and Ding et al. (2015), where CaO*= CaO-(10/3*P_2O_5). According to this approach, if the result is lower than the amount of Na_2O, the corrected value of CaO* is used in the CIA calculation; on the other hand, if the result is higher than the amount of Na_2O, the working assumption is that CaO* is equal to Na_2O (Hossain et al., 2014). The CIA is expressed as a dimensionless number between 0 and 100, the latter representing extreme weathering (McLennan, 1993; McLennan et al., 1993; Fedo et al., 1995; Liu et al., 2007), under the general assumption that in arid environment bedrock weathering and erosion are dominated essentially by physical processes of progressive mechanical breakdown, with only negligible chemical alteration and dissolution (i.e. ion mobilization) by agents such as water, organic acids, etc. Values can be plotted along the vertical axis on the Al_2O_3-CaO*+Na_2O-K_2O (A-CN-K) ternary diagram (Fig. 9; Fedo et al., 1995; Rieu et al., 2007; Zhang et al., 2013; Nagarajan et al., 2015), which gives information on the original composition of the parent rocks as well as on the weathering path of the sediments.

The CIA values of sandstone samples from both the Mariño and La Pilona formations are low to moderate (Figs. 9 and 10) and indicate that sediments underwent poor to moderate weathering prior to final deposition (Nesbitt and Young, 1982). The lowest values (< 50) belong to deposits of the dominantly aeolian Unit C, where the abundance of plagioclase (mostly albite) is high, thus indicating that sands accumulated dominantly by aeolian processes were nearly unaffected by chemical alteration. Compositional units A, B and D have low and relatively constant CIA values. A marked increase is found between units D and E (at approximately 688 m through the stratigraphic column; Fig. 10) where CIA value ranges increase from 50-55 to 55-60. The La Pilona Formation marks another

increase in CIA, with values varying between 55 and 65 (Fig. 10). The overall trend upward through stratigraphy shows increasing values of CIA, indicating slight and gradual increase of the weathering signature in the composition of sandstones.

The mineralogical maturity of siliciclastic sedimentary rocks can be expressed by the Mineral Index of Alteration (MIA, Eq. 2; Rieu et al., 2007), which can be visualized along the vertical axis in the mineralogical quartz-plagioclase-K-feldspar diagram (Nesbitt, 1996; Fig. 9):

$$MIA = \left(\frac{quartz}{quartz + K.felspar + plagioclase}\right) \times 100 \quad (2)$$

Plotted values show a vertical trend toward increasing mineralogical maturity upward through stratigraphy. In particular, the progressive depletion of the plagioclase component might be related to increasing weathering intensity.

Calculating the relative abundance of alumina to other major oxides, the Index of Compositional Variability [ICV = (Fe_2O_3 + K_2O + Na_2O + CaO + MgO + MnO + TiO_2)/Al_2O_3] is applied to evaluate sandstone compositional maturity (Cox et al., 1995). Immature clastic rocks have values greater than 1 and are often derived from first-cycle sediments, in contrast with more mature sedimentary rocks (ICV < 1) associated with intense chemical weathering (Cullers and Podkovyrov, 2002) and/or recycling (Cox et al., 1995; Long et al., 2008; Ding et al., 2015). All samples present ICV values higher than 1 (Appendix 1), reflecting first-cycle deposition, in agreement with their syntectonic origin in proximity of the source orogen, and providing no indication for recycling.

4.5. Sr and Nd isotopes

Stratigraphic trends in the isotopic ratios ($^{87}Sr/^{86}Sr$ and $^{143}Nd/^{144}Nd$ also expressed as ε_{Nd}) for these elements were used to identify the affinity of sediments to the composition of the source rocks (Faure, 2001; Yang et al., 2007). Here, Sr and Nd isotopic data are interpreted in terms of the relative changes in their values, the purpose being to decipher the evolution of the igneous signal in sandstones. Absolute values of the isotopic ratios of Sr and Nd and their relation to the formation of the igneous material are beyond the scope of this study. Higher values for the $^{87}Sr/^{86}Sr$ ratio and lower for ε_{Nd} are regarded as indicating a contribution from igneous source rocks more felsic in composition.

Analytical results for the $^{87}Sr/^{86}Sr$ ratio on bulk samples vary from 0.704271 ± 0.000002 on Unit A to 0.709572 ± 0.000005 in Unit G (Fig. 10), with a general trend to increasing values upward through stratigraphy, and a superposed, sharper increase from Unit F to Unit G that might represent a sudden change in the average igneous composition of the source rocks. The sample from Unit B also shows a distinct peak at 0.705465 ± 0.000002. The ε_{Nd} values of the bulk samples show a sharp decrease from Unit A (4.2 – 5.1) to Unit B (2.5), followed by a progressively decreasing trend upward through stratigraphy, except for a peak on the first sample from Unit F (908 m). Samples from the La Pilona Formation (Unit G) show variable ε_{Nd} values, and overall the lowest ones (averaging -2.4).

4.6. Variability of sediment composition

Along the stratigraphic succession, the composition of the Mariño and La Pilona sandstones records the transformation of catchment bedrock lithologies into sediments through a variety of concomitant processes acting at different temporal and/or spatial scales (Hillier, 1995). The Principal Component Analysis (PCA) conducted on samples from the two formations aims at deciphering trends in sandstones compositional signatures (Zhang et al., 2013) and relating these to different allogenic and/or autogenic processes. A discrimination between these main process categories is important to

unravel the system-scale dynamics involved in sediment deposition and to attribute causal relationships when interpreting the sedimentary record.

Calcite plays an important role in the total compositional variability of the studied sandstones, but does not feature any specific trend as it is essentially a secondary, diagenetic component and its occurrence thus strongly depends on sediment porosity and permeability. Calcite and zeolite, as cements, are present in different proportions through the stratigraphic succession (Fig. 3) and are part of early diagenesis during initial burial of the sediments (Burley and Worden, 2003; Steel and Milliken, 2013). Their presence obscures information that might give insights on factors taking place at different temporal and spatial scales (Alarcon and Pinto, 2015). Hence, in order to avoid spurious compositional signals related to the presence of these secondary minerals, PCA calculations were performed on CaO-, calcite- and zeolite-free data.

The PCA performed on the main mineralogy of sandstone samples from the Mariño and the La Pilona formations shows that the first and second dimensions (PC1 and PC2; Fig. 11A) explain approximately 56 % of the total compositional variability. Muscovite, kaolinite, K-feldspar and quartz plot preferentially in the first dimension (PC1) and are antagonists of plagioclase minerals (albite and anorthite). Samples from the Mariño and La Pilona formations plot along the PC1 with a progressive trend upward in stratigraphy from positive towards negative loadings showing the depletion of plagioclases and an attendant increase in kaolinite, muscovite and K-feldspar. This suggests the influence of weathering, supported also by increasing CIA values and by the concomitant increase in kaolinite content (Figs. 3 and 10), and by an increasing compositional maturity upward through stratigraphy. Even with low to moderate values of CIA (on average between 50 and 60), PC1 shows the importance of the weathering signal on whole-rock composition of sandstones from the Mariño and La Pilona formations. The second dimension (PC2; Fig. 11A) is mostly represented by illite, smectite and chlorite as positive loadings, and by heavy minerals (amphibole, pyroxene and Fe-Ti-oxides) as negative loadings. PC2 shows the importance of the concentration of the main clay-

minerals and the heavy-minerals in the whole compositional variability. The scattered distribution of samples from units D to G along PC2 shows their composition to be strongly influenced by the sporadic concentration of clay- and heavy- minerals, probably related to autogenic fluctuating hydrodynamic conditions during transport and deposition (Piton et al., 2016).

The PCA performed on the major elements explains 72.2 % of total elemental variability of samples from the Mariño and La Pilona formations (Fig. 11B). The resulting calculation shows samples from units A and B to plot close to the MgO pole. Samples from Unit C plot toward Na_2O and Al_2O_3, showing the importance of these elements in defining their compositional signature and revealing the marked contrast of aeolian sandstones from the overall increasing weathering trend of the fluvial units seen in figure 11B. Units D, E and F are scattered along PC1 and PC2 (Fig. 11B) and do not show any affinities with particular elements. Samples from Unit G are mostly scattered along PC1, revealing the importance of the Fe_2O_3-TiO_2 pole and confirming the effect of heavy-mineral concentration (mostly Fe-To-oxides as placer deposits), particularly recurrent in samples from the La Pilona Formation.

5. Discussion

5.1. Controls on the weathering signal

Given the potential relevance of the weathering signal to the compositional variability of sandstones from the Mariño and the La Pilona formations (PC1; Fig. 11A), it is important to constrain the factors that might have influenced CIA values, blurring then the actual weathering signal.

In the A-CN-K diagram (Fig. 9), changes due only to increasing intensity of chemical weathering cause the samples to plot parallel to the A-CN join, along an ideal weathering trend (IWT), resulting in higher values of CIA (Rieu et al., 2007), the reason being that weathering and elimination of plagioclase from an original grain population is more rapid and effective than for K-feldspar (Nesbitt and Young, 1984; Nagarajan et al. 2015). Sandstones from the Cacheuta Basin follow a slightly

deviated trend from the IWT and are oriented towards the illite pole, in agreement with the upward increase in illite content through stratigraphy, highlighted by QEMSCAN® results (Fig. 3) and confirmed by XRD analyses. Deviation of the measured trend from the IWT may be due to hydrodynamic sorting during sediment transport and deposition, to potassium metasomatism during diagenesis (Fedo et al., 1995; Hossain et al., 2010; Roy and Roser, 2012), and/or to progressive changes in source-rock composition (Nesbitt and Young, 1984; Rieu et al., 2007; von Eynatten et al. 2012b; Garzanti and Resentini, 2016). The CIA trend of sandstones from the Mariño and the La Pilona formations however does not follow the pattern to be expected from hydrodynamic sorting (Rieu et al., 2007). Main changes in the CIA correspond neither to enrichment nor depletion in clay-minerals as a result of hydrodynamic sorting, which would bring samples to plot respectively towards or away from the Al_2O_3 pole (Rieu et al., 2007). However, sandstones from the La Pilona Formation show variable CIA values that are strongly influenced by clay-mineral content. Indeed the variability of the CIA values in the La Pilona Formation is very similar to that of the clay-mineral content (Fig. 10). Hence, the effects of weathering may be expressed in CIA variations through La Pilona Formation, but the hydrodynamic concentration of clays is interfering with it. Petrographic observations did not reveal any evidence for potassium metasomatism as described by Fedo et al. (1995), thus the deviation of the weathering trend is probably related to the general increase in K-feldspar content through stratigraphy (Fig. 3), and can be accounted for by mixing with detritus coming from K-feldspar-rich sources.

Weathering in sediment source areas is primarily controlled by allogenic factors, such as changes in climatic conditions and tectonic activity (Nesbitt et al., 1997; Nesbitt, 2003; Hren et al., 2007; Liu et al., 2007), and is considered to be at a steady-state condition when the mentioned controls do not undergo major changes. Hence, the effects of weathering in the composition of the sandstones remain unchanged over time (Nesbitt, 2003). When these pre-conditions are no longer steady, their change is expected to reflect on the geochemistry and mineralogy of derived sediments. Rates of

chemical weathering are substantially reduced during periods of active tectonism, when physical erosion prevails on the high-gradient, often unstable topography of uplifting source terrains, and early sediment routing through the system is more rapid (Nesbitt, 2003). Conversely, during periods of tectonic quiescence and supposedly with no change in climatic conditions, rates of chemical weathering are expected to increase in the catchment area (Nesbitt, 2003), owing to the longer exposure of more stable landscape elements and of associated bedrock and regolith.

Throughout the stratigraphic column, the CIA shows a marked increase from Unit D to Unit E at approximately 688 m (Fig. 10). Sedimentological features and magnetostratigraphic data (Irigoyen et al. 2000) suggest essentially uninterrupted accumulation of the Mariño Formation related to hinterland uplift and protracted basin subsidence, with no evidence for quiescence in tectonic activity and/or significant changes in sediment supply. According to Giambiagi et al. (2014), this time period (~15 – 12 Ma) was characterized by high rates of crustal shortening in the region and a notable increase in foreland-basin accommodation immediately to the east of the Aconcagua Fold and Thrust Belt, also recorded in the Alto Tunuyán Basin (Irigoyen et al., 2000; Giambiagi and Ramos, 2003) and most likely related to the eastward advance of the thrust front (Giambiagi et al., 2001; Giambiagi and Ramos, 2003; Kay et al., 2005; Giambiagi et al., 2009; Giambiagi et al., 2014). Furthermore, the effects of tectonics are reflected in sedimentary systems mostly over longer time spans (McCann and Saintot, 2003; Leeder, 2011), and it is therefore unlikely that tectonic quiescence was the main factor responsible for a change in weathering conditions reflected in the abrupt change in CIA values observed here.

Climate is recognized to exert a dominant control on chemical weathering (Chesworth, 1992; White and Blum, 1995; Fedo et al., 1997; Riebe et al., 2004; Rieu et al., 2007, Adams et al., 2011; Ding et al., 2015). The range in CIA values of sandstones from the Mariño and La Pilona formations consistently indicate arid to semi-arid climatic conditions at the time of deposition (Huang et al., 2014; Ding et al., 2015). The abrupt change of the CIA values and concomitant increase in kaolinite concentration

around 688 m (Fig. 3) is more likely to reveal a climatic change in the catchment area toward relatively more humid conditions.

Sandstones from the aeolian member of the Mariño Formation (compositional Unit C) have CIA values lower than 50, due to a high concentration of albite (Fig. 3). Clay-mineral concentrations in turn do not show any particular change that might have affected the CIA values in this unit (Fig. 10). Tripaldi and Limarino (2005) suggested that the development of Andean aeolian systems at these latitudes was controlled by a combination of climate aridification and tectonism. In the compositional units of the Mariño Formation dominated by alluvial deposition some samples show distinctive peaks in CIA values below 50 and above 60, related to changes in the relative proportion of clay-minerals in the sandstones due probably to hydrodynamic sorting. These samples strongly plot along the PC2 axis (Fig. 11A) and are considered as low-order deviations from the general trend driven by the weathering factor.

Over the whole succession, the CIA and the MIA display progressively increasing values through stratigraphy (Fig. 10) but their variations do not follow exactly the same pattern indicating that weathering was probably not the only factor affecting sandstone mineralogical maturity. Indeed, MIA values for incipiently weathered samples are also strongly dependent on the source rock lithology (Rieu et al., 2007). In fact, the increasing geochemical and mineralogical maturity, also observed in the increasing K_2O/Na_2O values through stratigraphy (Potter, 1978; Akarish and El-Gohary, 2008; Appendix 1), suggests a progressively increasing input of sediments enriched in quartz and K-feldspar from more acidic igneous sources.

5.2. Provenance compositional signal

Determining the main composition of the bedrock sources feeding a sedimentary basin involves documenting the compositional trends along the stratigraphic succession (Heller and Frost, 1988). However, given the elevated sampling resolution, it is difficult to pinpoint changes in detrital bedrock

sources related to specific geological formations from the catchment area because of the secondary mixing of source contributions that might be controlled by local physiography and tectonic history, hard to assess. Apparent changes in detrital sources, for example, may be due to the specific geomorphic events within the catchment area (fluvial capture, tectonic partitioning of drainage pathways, etc.), to progressive unroofing of different lithologies, and/or to interactions with adjacent catchments.

Petrographic observations and paleocurrent data from the Mariño and La Pilona formations indicate a constant sediment supply from western to northwestern sources during the Miocene (Irigoyen, 1997; Giambiagi and Ramos, 2003). Two main provenance signatures are recorded in the studied formations: Ca-rich and igneous. Both geochemistry and mineralogy show a carbonatic source feeding the sedimentary basin, indirectly evidenced by the presence of abundant calcitic cement in the samples through the sedimentary succession and also by the presence of calcareous grains in samples from Unit A. This Ca-rich signature is most likely related to input from the Mesozoic sedimentary units within the eastern Principal Cordillera (Fig. 1A; Cegarra and Ramos, 1996; Cristallini and Ramos, 2000; Alarcon and Pinto, 2015), confirmed by the petrographic data reported by Irigoyen (1997) and by analogy with the sedimentary infill of the coeval Alto Tunuyán Basin which comprises clasts originating from the Mesozoic sedimentary units (Giambiagi and Ramos, 2003). However, the volume of calcitic cement is strongly linked to the porosity and permeability of the sandstones, and cannot be relied upon for accurate provenance discrimination.

The second main provenance signature has an igneous component which is clearly dominant and better preserved. The A-CN-K diagram (Fig. 9) allows to recognize the original source rocks from which sediments were derived (Cullers and Podkovyrov, 2002; Zhang et al., 2013). Data for the Mariño and the La Pilona formations reported on the plagioclase-K-feldspar line suggest an average andesitic-dioritic composition for the less weathered sediments, in agreement with the Th/Sc vs. Zr/Sc diagram (Fig. 12; Roser and Korsch, 1999; Mongelli et al., 2006), which recognizes also a more basaltic compositions for the lower units (A and B). The Th/Sc ratio is commonly regarded as a robust

provenance indicator (Taylor and McLennan, 1985; McLennan et al., 1993; Rieu et al., 2007; Mishra and Sen, 2012) as it is not sensitive to remobilization during processes such as weathering, diagenesis and metamorphism (Spalletti et al., 2012). Thorium is an incompatible trace element enriched in felsic rocks, whereas scandium is a compatible trace element relatively abundant in mafic rocks (McLennan and Taylor, 1991; McLennan et al., 1993). In the Zr/Sc ratio the Zr is provided by zircons, and it is a good indicator for zircon enrichment due to sediment recycling processes (McLennan et al., 1993; Long et al., 2008). Sandstones from the Mariño and La Pilona formations show a strong positive correlation between both Th/Sc and Zr/Sc ratios (Fig. 12), suggesting that provenance was mainly controlled by source-rock composition and not significantly biased by recycling (Mongelli et al., 2006; Long et al., 2008), in agreement with ICV values higher than unity (Appendix 1) that are suggestive of first-cycle deposition from active tectonic settings (Long et al., 2008).

Both Th/Sc and Zr/Sc ratios display relatively low values in samples from intervals below the aeolian member, especially the Th/Sc ratio in Unit A (Fig. 10), suddenly increasing in Unit B and then C. The isotopic compositions of Sr and Nd in units A and B (Fig. 10) reflect a change from more primitive to relatively more evolved igneous sources. The anorthite content remains high during the deposition of these two units (Fig. 3), confirming a less evolved igneous composition; this is also supported by the abundance of clinopyroxene-rich lithic grains reported by Irigoyen (1997). Values of Th/Sc and Zr/Sc ratios indicate a stable composition during the deposition of units D, E and F, with few deviations indicative of local enrichment in heavy minerals (especially in sandstones from Unit F), most likely related to sediment-transport processes. However, a decrease in anorthite and the concomitant increase in K-feldspar content in Unit C (Fig. 3) concur to indicate a progressive acidification of igneous sources. No significant provenance change is recognized at 688 m along the stratigraphic column (Fig. 10).

A major change in the Th/Sc and Zr/Sc ratios is observed for samples from the La Pilona Formation, which tend to display high variability. Low values of these ratios are due to high concentrations of

certain trace elements (among them Sc) and sporadic enrichment in heavy-minerals, in particular Fe-Ti-oxides, in placer deposits. This sediment-transport-related change in whole-rock composition is well defined by PCA calculations (Figs. 11A and 11B), and its effect is the addition of compositional noise to the main provenance signal. Nevertheless, the increase in volcanic lithic grains of acidic composition (Irigoyen, 1997), the significantly low pyroxene concentration in all samples from the La Pilona Formation (Unit G; Fig. 3), and relatively high $^{87}Sr/^{86}Sr$ and low ε_{Nd} values (Fig. 10) compared to the Mariño Formation, are all indicative of an important change toward a relatively more evolved igneous source composition. The influence of grain size on sandstone isotopic composition (Meyer et al. 2011; von Eynatten et al. 2012b) has been accounted for by the field sampling strategy, targeted at fine- to medium-grained sandstones.

The progressive evolution through stratigraphy of the whole-rock isotopic composition towards relatively more compositionally evolved sources is gradual and in agreement with the progressive evolution of the petrographic signal for tectonic setting from island arc to active continental margin (Figs. 5 and 6), as well as with the increasing relative proportion of acidic compared to basic volcanic lithic grains (Irigoyen, 1997). This trend is confirmed also by the gradually increasing abundance of incompatible trace elements (Rb, Y, La, Nd) compared to the relatively stable abundance of compatible trace elements (V, Ni, Cu) through stratigraphy (Fig. 4).

The classical diagram for discrimination of igneous suites by Le Maitre et al. (1989) has been applied to the sedimentary rocks (Fig. 13; Alarcon and Pinto, 2015). On the basis of this volcanic rock classification, the samples have a sub-alkaline composition and mainly plot in the andesitic-dacitic field. However, this diagram should be applied with care, as CaO concentration due to high secondary calcite content in sandstones might bias the significance of compositional values, especially regarding the relative concentration of SiO_2. The igneous discrimination diagram Zr/TiO_2 vs Nb/Y of Winchester and Floyd (1977) has also been used to infer source rock composition from the

sedimentary record (Fig. 14; Fralick 2003; Pinto et al., 2004; Alarcon and Pinto, 2015). It relies on immobile elements while neglecting the SiO_2 and alkali content of the rocks.

Based on the diagrams of Le Maitre et al. (1989) and Winchester and Floyd (1977; Figs. 13 and 14), and regarding the poorly evolved signature of sandstones from the basal part of the Mariño Formation (units A and B) revealed by geochemical and isotopic compositions, the main source can probably be traced into the tholeiitic andesites and basalts of the Abanico Formation in the western Principal Cordillera (Fock Kunstmann, 2005). According to the structural model of Giambiagi et al. (2016), the Principal Cordillera was being uplifted during the Early Miocene. In the Zr/TiO_2 vs Nb/Y and Th/Sc vs Zr/Sc diagrams (Figs. 14 and 12, respectively) the bedrock source composition of Unit A is better represented because the relevant elements are less affected in their relative abundances by the high calcite content. The interlayered volcanic rocks from the Mesozoic sedimentary sequences of the eastern Principal Cordillera could also have acted as clastic sources (Figs. 13 and 14), as they also show a poorly evolved signature, being mostly basalts and andesites (Fock Kunstmann, 2005), and originate from the early phases of deformation of the AFTB, antecedent to the advance of the volcanic arc front. Compositional signatures of the Farellones Formation have a wide range but are also more evolved (Fig. 13), and as such the contribution of this unit as sediment source was probably less important at these times. The early sedimentation history of the basin was then probably related to the development of the volcanic arc system along the western Principal Cordillera (see also Giambiagi et al., 2016).

According to some authors, a peripheral forebulge might have isolated this part of the foreland basin during deposition of the aeolian member (Porras et al., 2016; and references therein), providing then more evolved terrigenous debris mostly from the dacitic-rhyodacitic Choiyoi Group (Kleiman and Japas, 2009) presently outcropping in the Frontal Cordillera. However, the geochemical signature of Unit C does not bear a compositional signature referable to the Choiyoi Group (Figs. 13 and 14). Any

sediment supply from this Group is likely to have been masked by more significant sediment volumes originating from the Principal Cordillera.

The topmost fluvial member of the Mariño Formation (compositional units D, E and F) shows a more stable detrital and hence source-rock composition (Figs. 12, 13 and 14), most likely related to the Farellones Formation and the Aconcagua Volcanic Complex (15.8 – 8.6 Ma), which present a similar andesitic composition. This inference is in agreement with a progressive eastward advance of the volcanic front of approximately 50 km from the Farellones Arc in the Middle Miocene (Charrier et al., 2014).

Sandstone samples from the La Pilona Formation have very variable composition (Figs. 13 and 14), possibly reflecting an additional contribution from the Choiyoi Group, in the Frontal Cordillera, evident also from the increase in acidic lithic grains from petrographic observations (Irigoyen, 1997) and from the abundance of clasts sourced from the Frontal Cordillera reported in clast counts of conglomerates from the La Pilona Formation (Chiaramonte et al., 2000). However, the exact provenance of the sand fraction from the La Pilona Formation is difficult because the compositional signal related to source-rock composition is masked by the effects of heavy-mineral concentrations (mostly Fe-Ti oxides) as placer deposits within laminae of sampled sandstone strata. According to Irigoyen et al. (2000), the La Pilona Formation is chronologically correlated with the exhumation of the Frontal Cordillera, northwest of the study area. Moreover, Giambiagi and Ramos (2003) and Porras et al. (2016) acknowledge the occurrence of clasts in the coeval Palomares Formation of the Alto Tunuyan Basin sourced from the Frontal Cordillera during the break-up phase of the foreland (ca. 12-10 Ma).

5.3. Autogenic processes: discrimination and relevance

The observed variations in the whole-rock geochemistry and mineralogy through the studied succession result from the concomitant operation of source-area history (tied to both regional

tectonics and climate) and autogenic processes inherent to the dynamics of the depositional system responsible for the final sediment accumulation. Autogenic processes acting at system scale (e.g. Kim et al., 2006; Yoshida et al., 2007; Hajek et al., 2010; Ventra and Nichols, 2014) can influence variations in sediment distribution and composition, and thus the sedimentological interpretation of a basin fill, adding a potential complication in evaluating the role of allogenic forcing (Jerolmack and Paola, 2007, 2010).

As described above (section 2.2), the studied succession shows a progressive change in alluvial facies and architectures from the lower member of the Mariño Formation upward and into the La Pilona Formation, from relatively finer-grained, sandstone-dominated channel fills preserved within relatively large volumes of mudstone-rich alluvium representing overbank deposition, up to coarser-grained and increasingly amalgamated, gravel-dominated, thicker channel fills of the La Pilona Formation, accompanied by only sporadic preservation of residual overbank mudstones. In the absence of a direct influence from sea level, spatial and vertical changes in the architecture of fluvial deposits in continental foreland basins are commonly ascribed to relative changes between sediment supply and accommodation, generating a spectrum of stratigraphic architectures that ultimately relate to local variable preservation vs bypass potential for alluvial sediment (Currie, 1997; Martinsen et al., 1999; Kjemperud et al., 2008). However, the vertical architectural trends noted here are fully consistent with those described for the long-term evolution of stratigraphic records accumulated by fluvial fans (e.g. Atchley et al., 2013; Weissmann et al., 2013; Owen et al., 2015), in which fan progradation results in deposition of overbank-prone stratasets with relatively minor volumes of fine-grained channel fills, deposited on distal sectors, successively overlain by progressively coarser deposits from higher-gradient, more competent channel belts which tend to amalgamate their infills on the proximal fan domain. This essentially autogenic mechanism generates a stratigraphic coarsening trend and an upward increase in channel-to-overbank volume ratios in alluvial strata, linked to the spatial properties of distally widening distributive fluvial networks, whereby broader distal-fan surfaces consent preservation of greater relative volumes of overbank fines, whereas more

restricted proximal-fan surfaces are increasingly susceptible to reworking by avulsive channel belts (Davidson et al., 2013).

The autogenic origin of this vertical architectural trend through the Mariño-La Pilona system is confirmed: 1) by the vertical (i.e. temporal) persistence of alluvial and aeolian facies associations related to (semi)arid climate, indicating no significant climate change during the aggradational history (confirmed also by consistently low CIA values through the stratigraphic column); and 2) by a lack of evidence for abrupt changes in clastic sources over the time span comprised by the succession, showing a progressive compositional evolution, indicating that the effects of hinterland tectonics were probably gradual relatively to local rates of aggradation, and did not halt or reset the progradational evolution of the alluvial wedge. This further suggests that high-resolution compositional analyses of alluvial successions can provide an added criterion to verify the autogenic origin of stratigraphic styles attributable to fluvial-fan progradation, supporting a positive case when sediment geochemical and petrographic trends are relatively constant or otherwise gradually varying through particularly thick stratigraphic records (i.e. from many hundreds to over a thousand metres thick, and possibly more), aiding in the identification of fluvial-fan records in continental basin fills, which is still subject to debate (Sambrook Smith et al., 2010; Weissmann et al., 2010; Fielding et al., 2012).

In this framework it is also possible to explain the minor deviations from average sediment composition in the upper Mariño and La Pilona formations, ascribed to hydrodynamic sorting effects related to the autogenic change of depositional dynamics of fluvial channels (Piton et al., 2016). These uppermost stratigraphic units can be interpreted as the products of proximal, high-discharge and high-gradient channel belts, where relatively more competent tractive currents and/or more concentrated sediment dispersions would have been able to mix denser, ‘heavy’ minerals within bedload upon final deposition (Reid and Frostick, 1985; Garzanti and Andó, 2007). The occurrence of primary heavy-mineral fractions segregated especially in proximal channel fills of fluvial-fan deposits

has been noted previously (McGowen and Groat, 1971), and is probably an additional compositional trait inherent to fluvial patterns of hydrodynamic sorting to be accounted for when deriving information from compositional analyses of successions aggraded by such systems.

6. Summary and conclusions

Previous research on the Mariño and La Pilona formations in the central Argentinian foreland has established their contemporaneity with deposition in the Alto Tunuyán Basin. This work provides the first systematic compositional study of these formations in the Cacheuta Basin, corresponding to the distal segment of the broken foreland system. The evaluation of geochemical, mineralogical and isotopic data allows to characterise compositional variability through the fluvio-aeolian basin infill, and to relate such variability to allogenic forcing: i) the gradual increase in weathering conditions probably caused by slight climatic changes; ii) the sequential uplift of the Principal and Frontal Cordilleras during the Miocene. The multiproxy methodology adopted for this study also allowed pinpointing possible spurious compositional signals due to associated sedimentological, diagenetic and autogenic factors.

Sedimentological evidence indicates that the Mariño and La Pilona formations result from the progradational evolution of a fluvial-fan system over the western margin of the foreland basin, and were linked to Miocene development of the Andes in the region. Sediment composition through the studied succession shows a progressive change in bedrock sources from more primitive igneous lithotypes, mostly basaltic-andesitic (compositional units A and B), to relatively more evolved, andesitic-dacitic lithologies (compositional units C to F), related to the uplift of the western part of the Principal Cordillera, magmatic-arc evolution and sequential eastward advance of Andean thrust and volcanic fronts at these latitudes.

The aeolian member of the Mariño Formation (compositional Unit C) indicates interruption of fluvial-fan progradation during the establishment of an erg system in the early, underfilled phase of foreland history, possibly related to increased aridification (as shown by low CIA values; Fig. 10). A

relatively wide extent for the erg system is implied by the preservation of roughly coeval aeolian deposits along the Andean foreland system. First stages of uplift of the Frontal Cordillera are testified by sandstone compositional signals in the La Pilona Formation, at the top of the succession, but are partly blurred by the effect of depositional and autogenic processes. The unconformity at the transition between the Mariño and the La Pilona formations is most likely related to eastward advance of the deformation front, during early uplift of the Frontal Cordillera, as confirmed by chronological constraints and by compositional signals probably related to the Choiyoi Group preserved in samples from the La Pilona Formation. Sandstones from the late Mariño and especially La Pilona formations present isolated deviations from average compositional signals due to localized variations in the abundance of heavy minerals and clay minerals, most likely related to hydrodynamic segregation at deposition, and thus autogenic in origin. CIA values indicate quite stable, arid to semiarid climate throughout the entire succession, but suggest a possible shift to relatively more humid conditions during deposition of the Mariño Formation, between units D and E.

Overall, the relatively homogeneous mineralogical and geochemical composition through the stratigraphic column and its gradual trends toward the top part indicate continuity in the sedimentation history within the interpreted framework of progradation of a fluvial-fan system affected by hinterland tectonics. Large-scale trends in vertical facies abundance and architecture through the alluvial strata are likely related to the inherent tendency of fluvial fans to preserve and increasingly amalgamate coarse channel-belt and channel-fill deposits on their proximal domain. The compositional data documented here thus strongly support the role of a system-scale autogenic mechanism in governing the alluvial architecture in the Cacheuta Basin, supporting current hypotheses for the interpretation of some upward-coarsening alluvial successions as products of long-term activity of distributive fluvial systems, and possibly offering an additional criterion for the identification of such systems in the rock record.

Acknowledgements

This project was financed by the Swiss National Science Foundation, grant n° 200021_146736 to A.M. We would like to thank Michèle Senn for the isotopic analyses, François Gischig for the thin-section preparation, Fabio Capponi for the XRF measurements, as well as Branimir Segvic and Antoine De Haller for the QEMSCAN® measurements. We are very grateful to Miguel and Piki for their hospitality and support in Las Carditas (Potrerillos) during our long fieldwork missions. The article was greatly improved by the constructive comments of two anonymous reviewers and volume editor Sebastien Bertrand.

References

Abels, H.A., Kraus, M.J., Gingerich, P.D., 2013. Precession-scale cyclicity in the fluvial lower Eocene Willwood Formation of the Bighorn Basin, Wyoming (USA). Sedimentology 60 (6), 1467-1483. doi:10.1111/sed.12039

Adams, J.S., Kraus, M.J., Wing, S.L., 2011. Evaluating the use of weathering indices for determining mean annual precipitation in the ancient stratigraphic record. Palaeogeography, Palaeoclimatology, Palaeoecology 309 (3-4), 358–366. doi:10.1016/j.palaeo.2011.07.004

Adeigbe, O.C., Jimoh, Y.A., 2013. Geochemical fingerprints; implication for provenance, tectonic and depositional settings of Lower Benue trough sequence, Southeastern Nigeria. Journal of Environmental and Earth Sciences 3 (10), 115–141.

Aitchinson, J., 1982. The statistical analysis of compositional data. Journal of the Royal Statistical Society, Series B (Methodological) 44 (2), 139-177. doi:lO.1007i978-94-009-4109-0

Akarish, A.I.M., El-Gohary, A.M., 2008. Petrography and geochemistry of lower Paleozoic sandstones, East Sinai, Egypt: Implications for provenance and tectonic setting. Journal of African Earth Sciences 52 (1-2), 43–54. doi:10.1016/j.jafrearsci.2008.04.002

Alarcon, P., Pinto, L., 2015. Neogene erosion of the Andean Cordillera in the flat-slab segment as indicated by petrography and whole-rock geochemistry from the Manantiales Foreland Basin (32°-32°30'S). Tectonophysics 639 (12), 1–22. doi:10.1016/j.tecto.2014.11.001

Alessandretti, L., Philipp, R.P., Chemale, F., Brückmann, M.P., Zvirtes, G., Matté, V., Ramos, V.A., 2013. Provenance, volcanic record, and tectonic setting of the Paleozoic Ventania Fold Belt and the Claromecó Foreland Basin: Implications on sedimentation and volcanism along the southwestern Gondwana margin. Journal of South American Earth Sciences 47, 12–31. doi:10.1016/j.jsames.2013.05.006

Allen, J.L., Johnson, C.L., Heumann, M.J., Gooley, J., Gallin, W., 2012. New technology and methodology for assessing sandstone composition : A preliminary case study using a quantitative electron microscope scanner (QEMScan). In: Troy, E.R., Hemming, S.R., Riggs, N.R. (Eds.), Mineralogical and geochemical approaches to provenance, The Geological Society of America, Special Paper 487, pp. 177–194. doi:10.1130/2012.2487(11).

Allen, J.P., Fielding, C.R., 2007. Sedimentology and stratigraphic architecture of the Late Permian Betts Creek Beds, Queensland, Australia. Sedimentary Geology 202 (1-2), 5–34. doi:10.1016/j.sedgeo.2006.12.010

Álvarez, O., Lince Klinger, F., Gimenez, M., Ruiz, F., Martinez, P., 2016. Density and thermal structure of the Southern Andes and adjacent foreland from 32° to 55°S using earth gravity field models. In: Folguera, A., Naipauer, M., Sagripanti, L., Ghiglione Matías C, Orts, D.L., Giambiagi, L. (Eds.), Growth of the Southern Andes. Springer International Publishing, pp. 9–31. doi:10.1007/978-3-319-23060-3

Amorosi, A., Zuffa, G.G., 2011. Sand composition changes across key boundaries of siliciclastic and hybrid depositional sequences. Sedimentary Geology 236 (1-2), 153–163. doi:10.1016/j.sedgeo.2011.01.003

Atchley, S.C., Nordt, L.C., Dworkin, S.I., Cleveland, D.M., Mintz, J.S., Harlow, R.H., 2013. Alluvial stacking pattern analysis and sequence stratigraphy: concepts and case studies. In: Driese, S.G., Nordt, L.C. (Eds.), New frontiers in paleopedology and terrestrial paleoclimatology: paleosols ans soil surface analog systems, Society of Economic Paleontologists and Mineralogists, Special Publication 104, pp. 109-129. doi:10.2110/sepmsp.104.13.

Ballato, P., Strecker, M.R., 2014. Assessing tectonic and climatic causal mechanisms in foreland-basin stratal architecture: Insights from the Alborz Mountains, northern Iran. Earth Surface Processes and Landforms 39 (1), 110–125. doi:10.1002/esp.3480

Béguelin, P., Chiaradia, M., Beate, B., Spikings, R., 2015. The Yanaurcu volcano (Western Cordillera, Ecuador): A field, petrographic, geochemical, isotopic and geochronological study. Lithos 218–219, 37–53. doi:10.1016/j.lithos.2015.01.014

Bhatia, M.R., 1983. Plate tectonics and geochemical compositions of sandstones. The Journal of Geology 91 (6), 611–627. doi:10.1086/628815

Bhatia, M.R., Crook, K.A.W., 1986. Trace element characteristics of graywackes and tectonic setting discimination of sedimentary basins. Contributions to Mineralogy and Petrology 92 (2), 181–193. doi: 10.1007/BF00375292

Billi, P., 2008. Bedforms and sediment transport processes in the ephemeral streams of Kobo Basin, northern Ethiopia. Catena 75 (1), 5-17. doi:10.1016/j.catena.2008.04.002

Bridge, J.S., 2003. Rivers and floodplains. Blackwell Science, Oxford, UK. 491 p.

Buelow, E.K., Suriano, J., Mahoney, J.B., Mescua, J., Giambiagi, L., Kimbrough, D.L., 2014. Stratigraphic analysis of the neogene Cacheuta Basin: a record of orogenic exhumation and basin inversion in the South Central Andes. Geological Society of America, Annual Meeting Paper. Vols. 143-10 p. T126. Vancouver, 19-24 October 2014.

Burley, S., Worden, R., 2003. Sandstone diagenesis: recent and ancient. International Association Of Sedimentologists Reprint Series 4, 24. doi:10.1002/9781444304459

Cain, S.A., Mountney, N.P., 2009. Spatial and temporal evolution of a terminal fluvial fan system: the Permian Organ Rock Formation, south-east Utah, USA. Sedimentology 56 (6), 1774-1800. doi:10.1111/j.1365-3091.2009.01057.x

Cartigny, M.J.B., Ventra, D., Postma, G., Van Den Berg, J.H., 2014. Morphodynamics and sedimentary structures of bedforms under supercritical-flow conditions: new insights from flume experiments. Sedimentology 61 (3), 712-748. doi:10.1111/sed.12076

Cegarra, M.I., Ramos, V.A., 1996. La faja plegada y corrida del Aconcagua. In: Ramos, V.A. (Ed.), Geología de La Región Del Aconcagua, Provincias de San Juan Y Mendoza. Subsecretaría de Minería de la Nación, Dirección Nacional del Servicio Geológico, Buenos Aires. Anales, 24, pp. 387–422.

Cerdeño, E., Vucetich, M.G., 2007. The first rodent from the Mariño Formation (Miocene) at Divisadero Largo (Mendoza, Argentina) and its biochronological implications. Revista Geológica de Chile 34 (2), 199–207. doi:10.4067/S0716-02082007000200002

Charrier, R., Pinto, L., Rodriguez, M.P., 2007. Tectonostratigraphic evolution of the Andean Orogen in Chile. In: Moreno, T., Gibbons, W. (Eds.), The Geology of Chile. Geological Society of London, pp. 21–114. doi:10.1144/GOCH.3

Charrier, R., Ramos, V.A., Tapia, F., Sagripanti, L., 2014. Tectono-stratigraphic evolution of the Andean Orogen between 31 and 37° S (Chile and Western Argentina). In: Sepúlveda, S.A., Giambiagi, L.B., Moreiras, S.M., Pinto, L., Tunik, M., Hoke, G.D., Farías, M. (Eds.), Geodynamic processes in the Andes of Central Chile and Argentina, Geological Society, Special Publications 399, London, pp. 13–61. doi:10.1144/SP399.20

Chesworth, W., 1992. Weathering systems. In: Martini, I.P., Chesworth, W. (Eds.), Weathering, soils and paleosols, Developments in Earth Surface Processes 2. Elsevier, Amsterdam, pp. 19–40. doi:10.1016/B978-0-444-89198-3.50007-6

Chiaradia, M., Müntener, O., Beate, B., 2011. Enriched basaltic andesites from mid-crustal fractional crystallization, recharge, and assimilation (Pilavo volcano, Western Cordillera of Ecuador). Journal of Petrology 52 (6), 1107–1141. doi:10.1093/petrology/egr020

Chiaramonte, L., Ramos, V.A., Araujo, M., 2000. Estructura del anticlinal Barrancas, cuenca Cuyana, provincia de Mendoza. Revista de la Asociación Geológica Argentina 55, 309–336.

Covey, M., 1986. The evolution of foreland basins to steady state: evidence from the western Taiwan foreland basin. In: Allen, P.., Homewood, P. (Eds.), Foreland Basins, Special Publication of the International Association of Sedimentologists 8, pp. 77–90. doi:10.1002/9781444303810.ch4

Cox, R., Lowe, D.R., Cullers, R.L., 1995. The influence of sediment recycling and basement composition on evolution of mudrock chemistry in the southwestern United States. Geochimica et Cosmochimica Acta 59 (14), 2919–2940. doi:10.1016/0016-7037(95)00185-9

Cristallini, E.O., Ramos, V.A., 2000. Thick-skinned and thin-skinned thrusting in the La Ramada fold and thrust belt: Crustal evolution of the High Andes of San Juan, Argentina (32°SL). Tectonophysics 317 (3-4), 205–235. doi:10.1016/S0040-1951(99)00276-0

Crowley, K.D, 1983. Large-scale bed configurations (macroforms), Platte River Basin, Colorado and Nebraska: primary structures and formative processes. Geological Society of America Bulletin 94 (1), 117-133. doi:10.1130/0016-7606(1983)94<117:LBCMPR>2.0.CO;2

Cullers, R.L., Podkovyrov, V.N., 2002. The source and origin of terrigenous sedimentary rocks in the Mesoproterozoic Ui group, southeastern Russia. Precambrian Research 117 (3-4), 157–183. doi:10.1016/S0301-9268(02)00079-7

Currie, B.S., 1997. Sequence stratigraphy of nonmarine Jurassic-Cretaceous rocks, central Cordilleran foreland-basin system. Geological Society of America Bulletin 109 (9), 1206-1222. doi:10.1130/0016-7606(1997)109<1206:SSONJC>2.3.CO;2

Davidson, S.K., Hartley, A.J., Weissmann, G.S., Nichols, G.J., Scuderi, L.A., 2013. Geomorphic elements on modern distributive fluvial systems. Geomorphology 180-181, 82-95. doi: 10.1016/j.geomorph.2012.09.008

Dávila, F.M., Lithgow-Bertelloni, C., Giménez, M., 2010. Tectonic and dynamic controls on the topography and subsidence of the Argentine Pampas: The role of the flat slab. Earth and Planetary Science Letters 295 (1-2), 187–194. doi:10.1016/j.epsl.2010.03.039

DeCelles, P., 2012. Foreland basin systems revisited: variations in response to tectonic settings. In: Busby, C., Azor, A. (Eds.), Tectonics of Sedimentary Basins. John Wiley & Sons, Ltd, Chichester, UK, pp. 405–426. doi:10.1002/9781444347166.ch20

DeCelles, P.G., Cavazza, W., 1999. A comparison of fluvial megafans in the Cordilleran (Upper Cretaceous) and modern Himalayan foreland basin systems. Geological Society of America Bulletin 111 (9), 1315-1334. doi:10.1130/0016-7606(1999)111<1315:ACOFMI>2.3.CO;2

DeCelles, P.G., Giles, K.A., 1996. Foreland basin systems. Basin Research 8 (2), 105–123. doi:10.1046/j.1365-2117.1996.01491.x

DePaolo, D.J., Wasserburg, G.J., 1976a. Nd isotopic variations and petrogenetic models. Geophysical Research Letters 3 (5), 249–252. doi:10.1029/GL003i005p00249

DePaolo, D.J., Wasserburg, G.J., 1976b. Inferences about magma sources and mantle structure from variations of 143Nd/144Nd. Geophysical Research Letters 3 (12), 743–746. doi:10.1029/GL003i012p00743

Dewey, J.F., Bird, J.M., 1970. Mountain belts and the new global plate tectonics. Journal of Geophysical Research 75 (14), 2625–2647. doi:10.1029/JB075i014p02625

Dickinson, W.R., 1985. Interpreting provenance relations from detrital modes of sandstones. In: Zuffa, G.G. (Ed.), Provenance of Arenites. Springer Netherlands, pp. 333–361. doi:10.1007/978-94-017-2809-6_15

Dill, H.G., 1995. Heavy mineral response to the progradation of an alluvial fan: implications concerning unroofing of source area, chemical weathering and palaeo-relief (Upper Cretaceous Parkstein fan complex, SE Germany). Sedimentary Geology 95 (1), 39–56. doi:10.1016/0037-0738(94)00096-D

Ding, H., Ma, D., Yao, C., Lin, Q., Jing, L., 2015. Implication of the chemical index of alteration as a paleoclimatic perturbation indicator: an example from the lower Neoproterozoic strata of Aksu, Xinjiang, NW China. Geosciences Journal 20 (1), 13–26. doi:10.1007/s12303-015-0025-2

Dott, R.H., 1964. Wacke, graywacke, and matrix – What approach to immature sandstone classification? Journal of Sedimentary Petrology 34 (3), 625-632. doi:10.1306/74D71109-2B21-11D7-8648000102C1865D

Etemad-Saeed, N., Hosseini-Barzi, M., Armstrong-Altrin, J.S., 2011. Petrography and geochemistry of clastic sedimentary rocks as evidences for provenance of the Lower Cambrian Lalun Formation, Posht-e-badam block, Central Iran. Journal of African Earth Sciences 61 (2), 142–159. doi:10.1016/j.jafrearsci.2011.06.003

Faure, G., 2001. Chemical properties and isotope systematics. In: Faure, G. (Ed.), Origin of Igneous Rocks: The Isotopic Evidence. Springer, Berlin, Heidelberg, pp. 1–30. doi:10.1007/978-3-662-04474-2_1

Fedo, C.M., Nesbitt, H.W., Young, G.M., 1995. Unraveling the effects of potassium metasomatism in sedimentary rocks and paleosols, with implications for paleoweathering conditions and provenance. Geology 23 (10), 921–924. doi:10.1130/0091-7613(1995)023<0921:UTEOPM>2.3.CO;2

Fedo, C.M., Young, G.M., Nesbitt, H.W., 1997. Paleoclimatic control on the composition of the Paleoproterozoic Serpent Formation, Huronian Supergroup, Canada: a greenhouse to icehouse transition. Precambrian Research 86 (3-4), 201–223. doi:10.1016/S0301-9268(97)00049-1

Fielding, C.R., 2006. Upper flow regime sheets, lenses and scour fills: extending the range of architectural elements for fluvial sediment bodies. Sedimentary Geology 190 (1-4), 227-240. doi:10.1016/j.sedgeo.2006.05.009

Fielding, C.R., Ashworth, P.J., Best, J.L., Prokocki, E.W., Sambrook Smith, G.H., 2012. Tributary, distributary and other fluvial patterns: What really represents the norm in the continental rock record? Sedimentary Geology 261-262, 15-32. doi:10.1016/j.sedgeo.2012.03.004

Fock Kunstmann, A.I., 2005. Cronología y tectónica de la exhumación en el Neógeno de los Andes de Chile Central entre los 33° y los 34° S. (Master Thesis). Faculdad de Ciencias Físicas y Matemáticas, Universidad de Chile.

Fontana, A., Mozzi, P., Marchetti, M., 2014. Alluvial fans and megafans along the southern side of the Alps. Sedimentary Geology 301, 150-171. doi:10.1016/j.sedgeo.2013.09.003

Fordham, A.M., North, C.P., Hartley, A.J., Archer, S.G., Warwick, G.L., 2010. Dominance of lateral over axial sedimentary fill in dryland rift basins. Petroleum Geoscience 16 (3), 299-304. doi:10.1144/1354-079309-906

Fralick, P., 2003. Geochemistry of clastic sedimentary rocks: ratio techniques. In: Lentz, D.R. (Ed.), Geochemistry of sediments and sedimentary rocks: evolutionary considerations to mineral deposit-forming environments. Geological Association of Canada, Geotext 4, pp. 85–103.

Franco, M.J., Brea, M., Zavattieri, A.M., 2014. First record of fossil woods from the Mariño Formation (Miocene), Mendoza, Argentina and their palaeobiogeographical implications. Alcheringa 39 (1), 8–23. doi:10.1080/03115518.2014.951915

Fryberger, S.G., 1990. Role of water in eolian deposition. In: Fryberger, S.G., Krystinik, L.F., Schenk, C.J. (Eds.), Modern and ancient eolian deposits: petroleum exploration and production. Rocky Mountain Section, Society of Economic Paleontologists and Mineralogists, Denver (CO), pp. 41-52.

Garzanti, E., Andó, S., 2007. Heavy mineral concentration in modern sands: implications for provenance interpretation. In: Mange, M.A., Wright, D.T. (Eds.), Heavy Minerals in Use. Elsevier, Amsterdam, pp. 517-545. doi:10.1016/S0070-4571(07)58020-9

Garzanti, E., Resentini, A., 2016. Provenance control on chemical indices of weathering (Taiwan river sands). Sedimentary Geology 336, 81–95. doi:10.1016/j.sedgeo.2015.06.013

Giambiagi, L., Spagnotto, S., Moreiras, S.M., Gómez, G., Stahlschmidt, E., Mescua, J., 2015. Three-dimensional approach to understanding the relationship between the Plio-Quaternary stress field and tectonic inversion in the Triassic Cuyo Basin, Argentina. Solid Earth 6, 747–763. doi:10.5194/se-6-747-2015

Giambiagi, L., Tassara, A., Mescua, J., Tunik, M., Alvarez, P.P., Godoy, E., Hoke, G., Pinto, L., Spagnotto, S., Porras, H., Tapia, F., Jara, P., Bechis, F., García, V.H., Suriano, J., Moreiras, S.M., Pagano, S.D., 2014. Evolution of shallow and deep structures along the Maipo-Tunuyan transect (33 40'S): from the Pacific coast to the Andean foreland. In: Sepúlveda, S.., Giambiagi, L.., Moreiras, S.., Pinto, L., Tunik, M., Hoke, G.., Farías, M. (Eds.), Geodynamic processes in the Andes of Central Chile and Argentina, Geological Society, London, Special Publications, 399, pp. 63–82. doi:10.1144/SP399.14

Giambiagi, L., Tunik, M., Ramos, V.A., Godoy, E., 2009. The high andean Cordillera of Central Argentina and Chile along the Piuquenes pass-cordon del Portillo transect: Darwin's pioneering

observations compared with modern geology. Revista de la Asociación Geológica Argentina 64 (1), 43–54.

Giambiagi, L.B., Mescua, J., Bechis, F., Hoke, G., Suriano, J., Spagnotto, S., Moreiras, S.M., Lossada, A., Mazzitelli, M., Dapoza, R.T., Folguera, A., Mardonez, D., Pagano, D.S., 2016. Cenozoic orogenic evolution of the Southern Central Andes (32–36°S). In: Folguera, A., Naipauer, M., Sagripanti, L., Ghiglione Matías C, Orts, D.L., Giambiagi, L. (Eds.), Growth of the Southern Andes. Springer International Publishing, Cham, pp. 63–98. doi:10.1007/978-3-319-23060-3_4

Giambiagi, L.B., Ramos, V.A., 2003. Cenozoic deformation and tectonic style of the Andes, between 33° and 34° south latitude. Tectonics 22 (4), 1–18. doi:10.1029/2001TC001354

Giambiagi, L.B., Ramos, V.A., 2002. Structural evolution of the Andes in a transitional zone between flat and normal subduction (33°30'-33°45'S), Argentina and Chile. Journal of South American Earth Sciences 15 (1), 101–116. doi:10.1016/S0895-9811(02)00008-1

Giambiagi, L.B., Tunik, M.A., Ghiglione, M., 2001. Cenozoic tectonic evolution of the Alto Tunuyán foreland basin above the transition zone between the flat and normal subduction segment (33°30'–34°S), western Argentina. Journal of South American Earth Sciences 14 (7), 707–724. doi:10.1016/S0895-9811(01)00059-1

Gibling, M.R., 2006. Width and thickness of fluvial channel bodies and valley fills in the geological record: a literature compilation and classification. Journal of Sedimentary Research 76 (5), 731-770. doi:10.2110/jsr.2006.060

Goldberg, K., Humayun, M., 2010. The applicability of the Chemical Index of Alteration as a paleoclimatic indicator: An example from the Permian of the Paraná Basin, Brazil. Palaeogeography, Palaeoclimatology, Palaeoecology 293, 175–183. doi:10.1016/j.palaeo.2010.05.015

Govindaraju, K., 1994. 1994 Compilation of working values and sample description for 383 geostandards. Geostandards and Geoanalytical Research 18 (S1), 1–158. doi:10.1046/j.1365-2494.1998.53202081.x-i1

Gupta, S., 1997. Himalayan drainage patterns and the origin of fluvial megafans in the Ganges foreland basin. Geology 25 (1), 11-14. doi:10.1130/0091-7613(1997)025<0011:HDPATO>2.3.CO;2

Gutiérrez, P.R., Ottone, E.G., Japas, S.M. (Eds) 2006. Léxico Estratigráfico de la Argentina. Volumen VII, Pérmico. Asociación Geológica Argentina, Serie B 28, Servicio Geológico Minero Argentino. Buenos Aires, 167, 368 p.

Gutscher, M.A., 2002. Andean subduction styles and their effect on thermal structure and interplate coupling. Journal of South American Earth Sciences 15 (1), 3–10. doi:10.1016/S0895-9811(02)00002-0

Gutscher, M.A., Spakman, W., Bijwaard, H., Engdahl, E.R., 2000. Geodynamics of flat subduction: Seismicity and tomographic constraints from the Andean margin. Tectonics 19 (5), 814–833. doi:10.1029/1999TC001152

Hajek, E.A., Heller, P.L., Sheets, B.A., 2010. Significance of channel-belt clustering in alluvial basins. Geology 38 (6), 535-538. doi:10.1130/G30783.1

Hall, R., Smyth, H.R., 2008. Cenozoic arc processes in Indonesia: Identification of the key influences on the stratigraphic record in active volcanic arcs. In: Draut, A.E., Clift, D., Scholl, D.W. (Eds.), Formation and applications of the sedimentary record in arc collision zones, The Geological Society of America, Special Paper 436, pp. 27–54. doi:10.1130/2008.2436(03)

Hartley, A.J., Weissmann, G.S., Nichols, G.J., Warwick, G.L., 2010. Large distributive fluvial systems: characteristics, distribution, and controls on development. Journal of Sedimentary Research 80 (2), 167-183. doi:10.2110/jsr.2010.016

Hassan, M.A., 2005. Characteristics of gravel bars in ephemeral streams. Journal of Sedimentary Research 75 (1), 29-42. doi:10.2110/jsr.2005.004

Heller, P.L., Frost, C.D., 1988. Isotopic Provenance of clastic deposits: application of geochemistry to sedimentary provenance studies. In: Kleispehn, K., Paola, C. (Eds.), New Perspectives in Basin Analysis. Springer New York, pp. 27–42. doi:10.1007/978-1-4612-3788-4_2

Herron, M.M., 1988. Geochemical classification of terrigenous sands and shales from core or log data. Journal of Sedimentary Petrology 58 (5), 820–829. doi:10.1306/212F8E77-2B24-11D7-8648000102C1865D

Hillier, S., 1995. Erosion, sedimentation and sedimentary origin of clays. In: Velde, B. (Ed.), Origin and Mineralogy of Clays. Springer Berlin, pp. 162–246. doi:10.1007/978-3-662-12648-6_4

Hossain, H.M.Z., Roser, B.P., Kimura, J.I., 2010. Petrography and whole-rock geochemistry of the Tertiary Sylhet succession, northeastern Bengal Basin, Bangladesh: provenance and source area weathering. Sedimentary Geology 228 (3), 171–183. doi:10.1016/j.sedgeo.2010.04.009

Hossain, I., Roy, K.K., Biswas, P.K., Alam, M., Moniruzzaman, M., Deeba, F., 2014. Geochemical characteristics of Holocene sediments from Chuadanga district, Bangladesh: Implications for weathering, climate, redox conditions, provenance and tectonic setting. Chinese Journal of Geochemistry 33 (4), 336–350. doi:10.1007/s11631-014-0696-9

Hren, M.T., Hilley, G.E., Chamberlain, C.P., 2007. The relationship between tectonic uplift and chemical weathering rates in the Washington Cascades: Field measurements and model predictions. American Journal of Science 307 (9), 1041–1063. doi:10.2475/09.2007.01

Huang, J., Feng, L., Lu, D., Zhang, Q., Sun, T., Chu, X., 2014. Multiple climate cooling prior to Sturtian glaciations: evidence from chemical index of alteration of sediments in South China. Scientific reports 4, 6868. doi:10.1038/srep06868

Irigoyen, M.V., 1997. Magnetic polarity stratigraphy and geochronological constraints on the sequence of thrusting in the Principal and Frontal cordilleras and the Precordillera of the Argentine central Andes (33°S latitude). (PhD thesis) Carleton University, Ottawa.

Irigoyen, M. V, Buchan, K.L., Brown, R.L., 2000. Magnetostratigraphy of Neogene Andean foreland-basin strata, lat 33°S, Mendoza Province, Argentina. Geological Society of America Bulletin 112 (6), 803–816. doi:10.1130/0016-7606(2000)112<803:MONAFS>2.0.CO;2

Irigoyen, M. V, Buchan, K.L., Villeneuve, M.E., Brown, R.L., 2002. Cronología y significado tectónico de los estratos sinorogénicos neógenos aflorantes en la región de Cacheuta-Tupungato, Provincia de Mendoza. Revista de la Asociación Geológica Argentina 57, 3–18.

Jerolmack, D., Paola, C., 2007. Complexity in a cellular model of river avulsion. Geomorphology 91 (3-4), 259-270. doi:10.1016/j.geomorph.2007.04.022

Jerolmack, D.J., Paola, C., 2010. Shredding of environmental signals by sediment transport. Geophysical Research Letters 37, L19401. doi:10.1029/2010GL044638.

Jordan, T.E., 1981. Thrust loads and foreland basin evolution, Cretaceous, western United States. American Association of Petroleum Geologists Bulletin 65 (12), 2506–2520. doi:10.1306/03B599F4-16D1-11D7-8645000102C1865D

Jordan, T.E., 1995. Retroarc foreland basins. In: Busby, C.J., Ingersoll, R.V. (Eds.), Tectonics of sedimentary Basins. Blackwell Scientific Publications, Cambridge, pp. 331-362.

Jordan, T.E., Isacks, B.L., Ramos, V.A., Allmendinger, R.W., 1983a. Mountain building in the Central Andes. Episodes 3 (3), 20–26. doi:10.1029/JB094iB04p03891

Jordan, T.E., Isacks, B., Allmendinger, R.W., Brewer, J.A., Ramos, V.A., Ando, C.J., 1983b. Andean tectonics related to geometry of subducted Nazca Plate. Geological Society of America Bulletin 94 (3), 341-361. doi:10.1130/0016-7606(1983)94<341:ATRTGO>2.0.CO;2

Kay, S.M., Godoy, E., Kurtz, A., 2005. Episodic arc migration, crustal thickening, subduction erosion, and magmatism in the south-central Andes. Geological Society of America Bulletin 117 (1-2), 67–88. doi:10.1130/B25431.1

Kim, W.C., Paola, C., Swenson, J., Voller, V., 2006. Shoreline response to autogenic processes of sediment storage and release in fluvial systems. Journal of Geophysical Research 111, F04013. doi:10.1029/2006JF000470

Kjemperud, A.V., Schomacker, E.R., Cross, T.A., 2008. Architecture and stratigraphy of alluvial deposits, Morrison Formation (Upper Jurassic), Utah. American Association of Petroleum Geologists Bulletin 92 (8), 1055-1076. doi:10.1306/03250807115

Kleiman, L.E., Japas, M.S., 2009. The Choiyoi volcanic province at 34°S-36°S (San Rafael, Mendoza, Argentina): Implications for the Late Palaeozoic evolution of the southwestern margin of Gondwana. Tectonophysics 473 (3), 283–299. doi:10.1016/j.tecto.2009.02.046

Kokogian, D.A., Mancilla, O., 1989. Análisis estratigráfico secuencial de la Cuenca Neuquina. In: Chebli, G.., Spalletti, L.. (Eds.), Cuencas Sedimentarias Argentinas. Serie de Correlación Geológica, San Miguel de Tucumán, pp. 221–243.

Kocurek, G., Dott, R.H., 1981. Distinctions and uses of stratification types in the interpretation of eolian sand. Journal of Sedimentary Petrology 51, 579-595. doi:10.1306/212F7CE3-2B24-11D7-8648000102C1865D

Kocurek, G., Havholm, K.G., 1993. Eolian sequence stratigraphy – a conceptual framework. In: Weimer, P., Posamentier, H. (Eds.), Recent advances in and applications of siliciclastic sequence stratigraphy, American Association of Petroleum Geologists Memoir 58, Tulsa, pp. 393-409.

Kraus, M.J., Hasiotis, S.T., 2006. Significance of different modes of rhizolith preservation to interpreting paleoenvironmental and paleohydrologic settings: examples from Paleogene paleosols,

Bighorn Basin, Wyoming, U.S.A. Journal of Sedimentary Research 76 (4), 633-646. doi:10.2110/jsr.2006.052

Kraus, M.J., Riggins, S., 2007. Transient drying during the Paleocene-Eocene Thermal Maximum (PETM): Analysis of paleosols in the bighorn basin, Wyoming. Palaeogeography, Palaeoclimatology, Palaeoecology 245 (3), 444–461. doi:10.1016/j.palaeo.2006.09.011

Lancaster, N., Teller, J.T., 1988. Interdune deposits of the Namib Sand Sea. Sedimentary Geology 55 (1), 91-107. doi:10.1016/0037-0738(88)90091-7

Laronne, J.B., Shlomi, Y., 2007. Depositional character and preservation potential of coarse-grained sediments deposited by flood events in hyper-arid braided channels in the Rift Valley, Arava, Israel. Sedimentary Geology 195 (1-2), 21-37. doi:10.1016/j.sedgeo.2006.07.008

Lê, S., Josse, J., Husson, F., 2008. FactoMineR: an R package for multivariate analysis. Journal of Statistical Software 25 (1), 1–18. doi:10.18637/jss.v025.i01

Le Maitre, R.W., Baterman, P., Dudek, P., Séller, J., Lameyre Le Bas, J., Sabine, P.A., Schmid, R., Sorensen, H., Streckeisen, A., Woolley, A.R., Zanettin, B., 1989. A classification of igneous rocks and glossary of terms: recommendations of the International Union of Geological Sciences Subcommission on the Systematics of Igneous Rocks. Blackwell Scientific Publications, Oxford 193.

Leeder, M.R., 2011. Tectonic sedimentology: Sediment systems deciphering global to local tectonics. Sedimentology 58 (1), 2–56. doi:10.1111/j.1365-3091.2010.01207.x

Liu, B., Coulthard, T.J., 2015. Mapping the interactions between rivers and sand dunes: implications for fluvial and aeolian geomorphology. Geomorphology 231, 246-257. doi:10.1016/j.geomorph.2014.12.011

Liu, Z., Colin, C., Huang, W., Phon Le, K., Tong, S., Chen, Z., Trentesaux, A., 2007. Climatic and tectonic controls on weathering in south China and Indochina Peninsula: Clay mineralogical and geochemical

investigations from the Pearl, Red, and Mekong drainage basins. Geochemistry, Geophysics, Geosystems 8 (5), 1–18. doi:10.1029/2006GC001490

Llambías, E.J., Quenardelle, S., Montenegro, T., 2003. The Choiyoi Group from central Argentina: A subalkaline transitionalto alkaline association in the craton adjacent to the active marginof the Gondwana continent. Journal of South American Earth Sciences 16 (4), 243–257. doi:10.1016/S0895-9811(03)00070-1

Long, D.G.F., 2002. Aspects of Late Palaeoproterozoic fluvial style: the Uairén Formation, Roraima Supergroup, Venezuela. In: Altermann, W., Corcoran, P.L. (Eds.) Precambrian Sedimentary Environments: A Modern Approach to Ancient Depositional Systems. International Association of Sedimentologists, Special Publication 33, pp. 323-338. doi:10.1002/9781444304312.ch14

Long, D.G.F., 2017. Evidence of flash floods in Precambrian gravel dominated ephemeral river deposits. Sedimentary Geology 347, 53-66. doi:10.1016/j.sedgeo.2016.11.006

Long, X., Sun, M., Yuan, C., Xiao, W., Cai, K., 2008. Early Paleozoic sedimentary record of the Chinese Altai: Implications for its tectonic evolution. Sedimentary Geology 208 (3), 88–100. doi:10.1016/j.sedgeo.2008.05.002

Lowe, D.G., Arnott, R.W.C., 2016. Composition and architecture of braided and sheetflood-dominated ephemeral fluvial strata in the Cambrian-Ordovician Potsdam Group: a case example of the morphodynamics of early Phanerozoic fluvial systems and climate change. Journal of Sedimentary Research 86 (6), 587-612. doi:10.2110/jsr.2016.39

Manea, V.C., Pérez-Gussinyé, M., Manea, M., 2012. Chilean flat slab subduction controlled by overriding plate thickness and trench rollback. Geology 40 (1), 35–38. doi:10.1130/G32543.1

Martinsen, O.J., Ryseth, A., Helland-Hansen, W., Flesche, H., Torkildsen, G., Idil, S., 1999. Stratigraphic base level and fluvial architecture: Ericson Sandstone (Campanian), Rock Springs Uplift, SW Wyoming, USA. Sedimentology 46 (2), 235-259. doi:10.1046/j.1365-3091.1999.00208.x

McArthur, J.M., Howarth, R.J., Bailey, T.R., 2001. Strontium isotope stratigraphy: LOWESS version 3: best fit to the marine Sr-isotope curve for 0-509 Ma and accompanying look-up table for deriving numerical age. The Journal of Geology 109 (2), 155–170. doi:10.1086/319243

McCann, T., Saintot, A., 2003. Tracing tectonic deformation using the sedimentary record: an overview. In: McCann, T., Saintot, A. (Eds.), Tracing tectonic deformation using the sedimentary record, Geological Society, London, Special Publications 208, pp. 1–28. doi:10.1144/GSL.SP.2003.208.01.01

McGowen, J.H., Groat, C.G., 1971. Van Horn Sandstone, West Texas: an alluvial fan model for mineral exploration. Texas Bureau of Economic Geology, Report of Investigations 72, 57 p.

McLennan, S.M., 1993. Weathering and global denudation. The Journal of Geology 101 (2), 295–303. doi:10.1086/648222

McLennan, S.M., Hemming, S., McDaniel, D.K., Hanson, G.N., 1993. Geochemical approaches to sedimentation, provenance, and tectonics. In: Johnsson, M.J., Basu, A. (Eds.), Processes controlling the composition of clastic sediments, Geological Society of America, Special Paper 284, pp. 21–40. doi:10.1130/SPE284-p21

McLennan, S.M., Taylor, S.R., 1991. Sedimentary rocks and crustal evolution: tectonic setting and secular trends. The Journal of Geology 99 (1), 1–21. doi:10.1086/629470

Meyer, I., Davies, G.R., Stuut, J.-B.W., 2011. Grain size control on Sr-Nd isotope provenance studies and impact on paleoclimate reconstructions: An example from deep-sea sediments offshore NW Africa. Geochemistry, Geophysics, Geosystems 12 (3). doi:10.1029/2010GC003355

Miall, A.D., 1985. Architectural-element analysis: a new method of facies analysis applied to fluvial deposits. Earth-Science Reviews 22, 261-308. doi:10.1016/0012-8252(85)90001-7

Miall, A.D., 2014. Fluvial Depositional Systems. Springer International Publishing, 316 pp.

Milana, J.P., Cevallos, M.F., Zavattieri, A.M., Prampano, M., Papu, H.O., 1993. La secuencia terciaria de Pachaco: sedimentologia, edad, correlaciones y significado paleogeografico. XII Congreso Geológico Argentino and II Congreso de Exploración de Hidrocarburos. Actas I, 226–234.

Mishra, M., Sen, S., 2012. Provenance, tectonic setting and source-area weathering of Mesoproterozoic Kaimur Group, Vindhyan Supergroup, Central India. Geologica Acta 10 (3), 283–293. doi:10.1344/105.000001759

Mongelli, G., Critelli, S., Perri, F., Sonnino, M., Perrone, V., 2006. Sedimentary recycling, provenance and paleoweathering from chemistry and mineralogy of Mesozoic continental redbed mudrocks, Peloritani mountains, southern Italy. Geochemical Journal 40 (2), 197–209. doi:10.2343/geochemj.40.197

Muñoz, M., Fuentes, F., Vergara, M., Aguirre, L., Olov Nyström, J., Féraud, G., Demant, A., 2006. Abanico East Formation: petrology and geochemistry of volcanic rocks behind the Cenozoic arc front in the Andean Cordillera, central Chile (33°50'S). Revista geológica de Chile 33 (1), 109–140. doi:10.4067/S0716-02082006000100005

Nagarajan, R., Armstrong-Altrin, J.S., Kessler, F.L., Hidalgo-Moral, E.L., Dodge-Wan, D., Taib, N.I., 2015. Provenance and tectonic setting of Miocene siliciclastic sediments, Sibuti formation, northwestern Borneo. Arabian Journal of Geosciences 8 (10), 8549–8565. doi:10.1007/s12517-015-1833-4

Nesbitt, H.W., 2003. Petrogenesis of siliciclastic sediments and sedimentary rocks. In: Geochemistry of Sediments and Sedimentary Rocks: Evolutionary Considerations to Mineral Deposit-Forming Environments. Geological Association of Canada, GeoText 4, pp. 39–51.

Nesbitt, H.W., Fedo, C.M., Young, G.M., 1997. Quartz and feldspar stability, steady and non-steady-state weathering, and petrogenesis of siliciclastic sands and muds. The Journal of Geology 105 (2), 173–191. doi:10.1086/515908

Nesbitt, H.W., Young, G.M., 1996. Petrogenesis of sediments in the absence of chemical weathering: effects of abrasion and sorting on bulk composition and mineralogy. Sedimentology 43 (2), 341–358. doi:10.1046/j.1365-3091.1996.d01-12.x

Nesbitt, H.W., Young, G.M., 1984. Prediction of some weathering trends of plutonic and volcanic rocks based on thermodynamic and kinetic considerations. Geochimica et Cosmochimica Acta 48 (7), 1523–1534. doi:10.1016/0016-7037(84)90408-3

Nesbitt, H.W., Young, G.M., 1982. Early Proterozoic climates and plate motions inferred from major element chemistry of lutites. Nature 299, 715–717. doi:10.1038/299715a0

Nichols, G.J., Fisher, J.A., 2007. Processes, facies and architecture of fluvial distributary system deposits. Sedimentary Geology 195 (1-2), 75–90. doi:10.1016/j.sedgeo.2006.07.004

Ohta, T., Arai, H., 2007. Statistical empirical index of chemical weathering in igneous rocks: A new tool for evaluating the degree of weathering. Chemical Geology 240 (3-4), 280–297. doi:10.1016/j.chemgeo.2007.02.017

Owen, A., Nichols, G.J., Hartley, A.J., Weissmann, G.S., Scuderi, L.A., 2015. Quantification of a distributive fluvial system : the Salt Wash DFS of the Morrison Formation, SW U.S.A. Journal of Sedimentary Research 85 (5), 544–561. doi:10.2110/jsr.2015.35

Owen, A., Ebinghaus, A., Hartley, A.J., Santos, M.G.M., Weissmann, G.S., 2017. Multi-scale classification of fluvial architecture: an example from the Palaeocene-Eocene Bighorn Basin, Wyoming. Sedimentology 64 (6), 1572-1596. doi:10.1111/sed.12364

Pe-Piper, G., Triantafyllidis, S., Piper, D.J.W., 2008. Geochemical identification of clastic sediment provenance from known sources of similar geology: the Cretaceous Scotian Basin, Canada. Journal of Sedimentary Research 78 (9), 595–607. doi:10.2110/jsr.2008.067

Pearce, T.J., Besly, B.M., Wray, D.S., Wright, D.K., 1999. Chemostratigraphy: A method to improve interwell correlation in barren sequences - a case study using onshore Duckmantian/Stephanian sequences (West Midlands, U.K.). Sedimentary Geology 124 (1), 197–220. doi:10.1016/S0037-0738(98)00128-6

Perez, D.J., 2001. Tectonic and unroofing history of Neogene Manantiales foreland basin deposits , Cordillera Frontal (32°30' S), San Juan Province , Argentina. Journal of South American Earth Sciences 14 (7), 693–705. doi:10.1016/S0895-9811(01)00071-2

Pettijohn, F.J., Potter, P.E., Siever, R., 1972. Sand and sandstone. Springer US, New York, pp. 618.

Pinto, L., Hérail, G., Moine, B., Fontan, F., Charrier, R., Dupré, B., 2004. Using geochemistry to establish the igneous provenances of the Neogene continental sedimentary rocks in the Central Depression and Altiplano, Central Andes. Sedimentary Geology 166 (1-2), 157–183. doi:10.1016/j.sedgeo.2003.12.002

Piton, G., Mejean, S., Carbonari, C., Guern, J.L.E., Bellot, H., Recking, A., 2016. Bedload trapping in open check dam basins-measurements of flow velocities and depositions patterns. 13th Congress INTERPRAEVENT 2016, Lucerne, Switzerland, pp. 808-817.

Polanski, J., 1958. El bloque varíscico de la Cordillera Frontal de Mendoza. Revista de la Asociación Geológica Argentina 12, 165–196.

Polanski, J., 1964. Descripción geológica de la hoja 25a-Volcan San José: Provincia de Mendoza. Dirección Nacional de Geología y Minería, Buenos Aires 1–92.

Porras, H., Pinto, L., Tunik, M., Giambiagi, L., Deckart, K., 2016. Provenance of the Miocene Alto Tunuyán Basin (33°40'S, Argentina) and its implications for the evolution of the Andean Range: Insights from petrography and U–Pb LA–ICPMS zircon ages. Tectonophysics 690, 298–317. doi:10.1016/j.tecto.2016.09.034

Potter, P.E., 1978. Petrology and chemistry of modern big river sands. The Journal of Geology 86 (4), 423–449. doi:10.1086/649711

Powell, D.M., 2009. Dryland rivers: Processes and forms. In: Parsons A.J., Abrahams A.D. (Eds.), Geomorphology of desert environments. Springer Science, Berlin, pp. 333-373. doi:10.1007/978-1-4020-5719-9_12

Price, J.R., Velbel, M.A., 2003. Chemical weathering indices applied to weathering profiles developed on heterogeneous felsic metamorphic parent rocks. Chemical Geology 202 (3-4), 397–416. doi:10.1016/j.chemgeo.2002.11.001

Price, R.A., 1973. Large-scale gravitational flow of supracrustal rocks, southern Canadian Rockies. In: DeJong, K., Scholten, R. (Eds.), Gravity and Tectonics. Wiley, New York, pp. 491–502.

Ramos, V.A., 2009. Anatomy and global context of the Andes : main geologic features and the Andean orogenic cycle. In: Kay, S.M., Ramos, V.A., Dickinson, W.R. (Eds.), Backbone of the Americas: shallow subduction, plateau uplift, and ridge and terrane collision, Geological Society of America Memoirs 204, pp. 31–65. doi:10.1130/2009.1204(02)

Ramos, V.A., Cegarra, M., Cristallini, E., 1996a. Cenozoic tectonics of the High Andes of west-central Argentina (30–36°S latitude). Tectonophysics 259 (1), 185–200. doi:10.1016/0040-1951(95)00064-X

Ramos, V.A., Cristallini, E.O., Pérez, D.J., 2002. The Pampean flat-slab of the Central Andes. Journal of South American Earth Sciences 15 (1), 59–78. doi:10.1016/S0895-9811(02)00006-8

Ramos, V.A., Kay, S.M., Perez, D.J., 1996b. El volcanismo de la región del Aconcagua. In: Ramos, V. (Ed.), Geología de la región del Aconcagua, provincias de San Juan Y Mendoza. Subsecretaría de Minería de la Nación, Dirección Nacional del Servicio Geológico, Buenos Aires. Anales, 24, pp. 297–316.

Reid, I., Frostick, L.E., 1985. Role of settling, entrainment and dispersive equivalence and of interstice trapping in placer formation. Journal of the Geological Society of London 142 (5), 739-746. doi:10.1144/gsjgs.142.5.0739

Reynolds, J.H., Jordan, T.E., Johnson, N.M., Damanti, J.F., Tabbutt, K.D., 1990. Neogene deformation of the flat-subduction segment of the Argentine-Chilean Andes: Magnetostratrigraphic constraints from Las Junta, La Rioja province, Argentina. Geological Society of America Bulletin 102 (12), 1607–1622. doi:10.1130/0016-7606(1990)102<1607

Riebe, C.S., Kirchner, J.W., Finkel, R.C., 2004. Erosional and climatic effects on long-term chemical weathering rates in granitic landscapes spanning diverse climate regimes. Earth and Planetary Science Letters 224 (3-4), 547–562. doi:10.1016/j.epsl.2004.05.019

Rieu, R., Allen, P.A., Plotze, M., Pettke, T., 2007. Compositional and mineralogical variations in a Neoproterozoic glacially influenced succession, Mirbat area, south Oman: Implications for paleoweathering conditions. Precambrian Research 154 (3-4), 248–265. doi:10.1016/j.precamres.2007.01.003

Roser, B.P., Korsch, R.J., 1999. Geochemical characterization, evolution and source of a Mesozoic accretionary wedge: the Torlesse terrane, New Zealand. Geological Magazine 136 (5), 493–512. doi:10.1017/S0016756899003003

Roser, B.P., Korsch, R.J., 1986. Determination of tectonic setting of sandstone-mudstone suites using SiO_2 Content and K_2O/Na_2O ratio. The Journal of Geology 94 (5), 635–650. doi:10.1086/629071

Rossetti, D.F., Zani, H., Cohen, M.C.L., Cremon, É.H., 2012. A Late Pleistocene-Holocene wetland megafan in the Brazilian Amazonia. Sedimentary Geology 282, 276-293. doi:10.1016/j.sedgeo.2012.09.015

Roy, D.K., Roser, B.P., 2012. Geochemistry of Tertiary sequence in Shahbajpur-1 well, Hatia Trough, Bengal Basin, Bangladesh: provenance, source weathering and province affinity. Journal of Life and Earth Sciences 7, 1–13. doi:10.3329/jles.v7i0.20115

Rust, B.R., Gibling, M.R., 1990. Braidplain evolution in the Pennsylvanian South Bar Formation, Sydney Basin, Nova Scotia, Canada. Journal of Sedimentary Petrology 60 (1), 59-72. doi:10.1306/212F9110-2B24-11D7-8648000102C1865D

Saitoh, Y., Tamura, T., Kodama, Y., Nakano, T., 2011. Strontium and neodymium isotopic signatures indicate the provenance and depositional process of loams intercalated in coastal dune sand, western Japan. Sedimentary Geology 236 (3), 272–278. doi:10.1016/j.sedgeo.2011.01.012

Sambrook Smith, G.H., Best, J.L., Ashworth, P.J., Fielding, C.R., Goodbred, S.L., Prokocki, E.W., 2010. Fluvial form in modern continental sedimentary basins: Distributive fluvial systems: Comment. Geology 38 (12), e230. doi:10.1130/G31507C.1

Schlunegger, F., Norton, K.P., 2015. Climate vs. tectonics: The competing roles of late Oligocene warming and Alpine orogenesis in constructing alluvial megafan sequences in the North Alpine foreland basin. Basin Research 27 (2), 230–245. doi:10.1111/bre.12070

Schlunegger, F., Matter, A., Burbank, D.W., Leu, W., Mange, M., Màtyàs, J., 1997. Sedimentary sequences, seismofacies and evolution of depositional systems of the Oligo/Miocene Lower

Freshwater Molasse Group, Switzerland. Basin Research 9 (1), 1-26. doi:10.1046/j.1365-2117.1997.00029.x

Sempere, T., Marshall, L.G., Rivano, S., Godoy, E., 1994. Late Oligocene-Early Miocene compressional tectosedimentary episode and associated land-mammal faunas in the Andes of central Chile and adjacent Argentina (32-37°S). Tectonophysics 229 (3), 251–264. doi:10.1016/0040-1951(94)90032-9

Shao, J., Yang, S., 2012. Does chemical index of alteration (CIA) reflect silicate weathering and monsoonal climate in the Changjiang River basin? Chinese Science Bulletin 57 (10), 1178–1187. doi:10.1007/s11434-011-4954-5

Smith, G.A., 1986. Coarse-grained nonmarine volcaniclastic sediment: terminology and depositional process. Geological Society of America Bulletin 97 (1), 1-10. doi:10.1130/0016-7606(1986)97<1:CNVSTA>2.0.CO;2

Spalletti, L.A., Limarino, C.O., Piñol, F.C., 2012. Petrology and geochemistry of Carboniferous siliciclastics from the Argentine Frontal Cordillera: A test of methods for interpreting provenance and tectonic setting. Journal of South American Earth Sciences 36, 32–54. doi:10.1016/j.jsames.2011.11.002

Stanistreet, I.G., Stollhofen, H., 2002. Hoanib river flood deposits of Namib Desert interdunes as analogues for thin permeability barrier mudstone layers in aeolianite reservoirs. Sedimentology 49 (4), 719-736. doi:10.1046/j.1365-3091.2002.00458.x

Stear, W.M., 1983. Morphological characteristics of ephemeral stream channel and overbank splay sandstone bodies in the Permian Lower Beaufort Group, Karoo Basin, South Africa. In: Collinson, J.D., Lewin, J. (Eds.), Modern and Ancient Fluvial Systems. Blackwell Publishing, Oxford, International Association of Sedimentologists, Special Publication 6, pp. 405-420. doi:10.1002/9781444303773.ch33

Steel, R.J., Milliken, K.L., 2013. Major Advances in siliciclastic sedimentary geology 1960-2012. In: Bickford, M.E. (Ed.), Web of geological sciences: advances, impacts, interactions, The Geological Society of America, Special Paper 500, pp. 121–167. doi:10.1130/2013.2500(04).

Strecker, M.R., Hilley, G.E., Bookhagen, B., Sobel, E.R., 2012. Structural, geomorphic, and depositional characteristics of contiguous and broken foreland basins: examples from the eastern flanks of the central Andes in Bolivia and NW Argentina. In: Busby, C., Azor, A. (Eds.), Tectonics of Sedimentary Basins: Recent Advances. Blackwell Publishing, Oxford, pp. 508-521. doi:10.1002/9781444347166.ch25

Suttner, L.J., Dutta, P.K., 1986. Alluvial sandstone composition and paleoclimate; I, Framework mineralogy. Journal of Sedimentary Research 56 (3), 329–345. doi:10.1306/212F8909-2B24-11D7-8648000102C1865D

Tanaka, T., Togashi, S., Kamioka, H., Amakawa, H., Kagami, H., Hamamoto, T., Yuhara, M., Orihashi, Y., Yoneda, S., Shimizu, H., Kunimaru, T., Takahashi, K., Yanagi, T., Nakano, T., Fujimaki, H., Shinjo, R., Asahara, Y., Tanimizu, M., Dragusanu, C., 2000. JNdi-1: A neodymium isotopic reference in consistency with LaJolla neodymium. Chemical Geology 168 (3-4), 279–281. doi:10.1016/S0009-2541(00)00198-4

Taylor, S.R., McLennan, S.M., 1985. The continental crust: its composition and evolution. An examination of the geochemical record preserved in sedimentary rocks. Blackwell, Oxford. pp.312.

Tripaldi, A., Limarino, C.O., 2005. Vallecito Formation (Miocene): The evolution of an eolian system in an Andean foreland basin (northwestern Argentina). Journal of South American Earth Sciences 19 (3), 343–357. doi:10.1016/j.jsames.2005.04.006

Uba, C.E., Heubeck, C., Hulka, C., 2006. Evolution of the late Cenozoic Chaco foreland basin, southern Bolivia. Basin Research 18 (2), 145-170. doi:10.1111/j.1365-2117.2006.00291.x

Van den Boogaart, K.G., Tolosana-Delgado, R., 2008. “compositions”: A unified R package to analyze compositional data. Computers & Geosciences 34 (4), 320–338. doi:10.1016/j.cageo.2006.11.017

Ventra, D., Nichols, G.J., 2014. Autogenic dynamics of alluvial fans in endorheic basins: outcrop examples and stratigraphic significance. Sedimentology 61 (3), 767-791. doi:10.1111/sed.12077

Vergara, M., Nystrom, J., 1996. Geochemical features of lower Cretaceous back-arc lavas in the Andean Cordillera, Central Chile (31-34°S). Revista Geológica de Chile 23 (1), 97–106. doi:10.5027/andgeoV23n1-a06

Von Eynatten, H., Critelli, S., Ingersoll, R. V, Wetlje, G.J., 2012a. Introduction to the special issue “Actualistic Models of Sediment Generation”. Sedimentary Geology 280 (1), 1–3. doi:10.1016/j.sedgeo.2012.07.020

Von Eynatten, H., Tolosana-Delgado, R., Karius, V., 2012b. Sediment generation in modern glacial settings : Grain-size and source-rock control on sediment composition. Sedimentary Geology, 280, 80–92. doi:10.1016/j.sedgeo.2012.03.008

Walcek, A.A., Hoke, G.D., 2012. Surface uplift and erosion of the southernmost Argentine Precordillera Range, constrained two ways. Geomorphology 153–154, 156–168. doi:10.1016/j.geomorph.2012.02.021

Wasserburg, G.J., Jacousen, S.B., DePaolo, D.J., McCulloch, M.T., Wen, T., 1981. Precise determination of Sm/Nd ratios, Sm and Nd isotopic abundances in standard solutions. Geochimica et Cosmochimica Acta 45 (12), 2311–2323. doi:10.1016/0016-7037(81)90085-5

Weissmann, G.S., Hartley, A.J., Nichols, G.J., Scuderi, L.A., Olson, M., Buehler, H., Banteah, R., 2010. Fluvial form in modern continental sedimentary basins: distributive fluvial systems. Geology 38 (1), 39–42. doi:10.1130/G30242.1

Weissmann, G.S., Hartley, A.J., Nichols, G.J., Scuderi, L.A., Olson, M.E., Buehler, H.A., Massengill, L.G., 2011. Alluvial facies distribution in continental sedimentary basins: distributive fluvial systems. In: Davidson, S., Leleu, S., North, C. (Eds.), From river to rock record: the preservation of fluvial sediments and their subsequent interpretation, Society of Economic Paleontologists and Mineralogists, Special Publication 97, pp. 327-355. doi:10.2110/sepmsp.097.327

Weissmann, G.S., Hartley, A.J., Scuderi, L.A., Nichols, G.J., Davidson, S.K., Owen, A., Atchley, S.C., Bhattacharyya, P., Chakraborty, T., Ghosh, P., Nordt, L.C., Michel, L., Tabor, N.J., 2013. Prograding distributive fluvial systems: geomorphic models and ancient examples. In: Driese, S.G., Nordt, L.C., McCarthy, P.J. (Eds.), New frontiers in paleopedology and terrestrial paleoclimatology, Society of Economic Paleontologists and Mineralogists, Special Publication 104, pp. 131–147. doi:10.2110/sepmsp.104.16

White, A.F., Blum, A.E., 1995. Effects of climate on chemical weathering in watersheds. Geochimica et Cosmochimica Acta 59 (9), 1729–1747. doi:10.1016/0016-7037(95)00078-e

Wilson, I.G., 1971. Desert sandflow basins and a model for the development of ergs. The Geographical Journal 137 (2), 180-199. doi:10.2307/1796738

Wilson, I.G., 1973. Ergs. Sedimentary Geology 10 (2), 77-106. doi:10.1016/0037-0738(73)90001-8

Winchester, J.A., Floyd, P.A., 1977. Geochemical discrimination of different magma series and their differentiation products using immobile elements. Chemical Geology 20, 325–343. doi:10.1016/0009-2541(77)90057-2

Yang, S., Jiang, S., Ling, H., Xia, X., Sun, M., Wang, D., 2007. Sr-Nd isotopic compositions of the Changjiang sediments : Implications for tracing sediment sources. Science in China Series D: Earth Sciences 50 (10), 1556–1565. doi:10.1007/s11430-007-0052-6

Yoshida, S., Steel, R.J., Dalrymple, R.W., 2007. Changes in depositional processes – An ingredient in a new generation of sequence-stratigraphic models. Journal of Sedimentary Research 77 (6), 447-460. doi:10.2110/jsr.2007.048

Yrigoyen, M.R., 1993. Los depositos sinorogenicos terciarios. XII Congreso Geológico Argentino and II Congreso de Exploración de Hidrocarburos. Actas I, 123–148.

Zaid, S.M., Elbadry, O., Ramadan, F., Mohamed, M., 2015. Petrography and geochemistry of Pharaonic sandstone monuments in Tall San Al Hagr , Al Sharqiya Governorate , Egypt : implications for provenance and tectonic setting. Turkish Journal of Earth Sciences 24 (4), 344–364. doi:10.3906/yer-1407-20

Zhang, Y., Pe-Piper, G., Piper, D.J.W., 2013. Sediment geochemistry as a provenance indicator: Unravelling the cryptic signatures of polycyclic sources, climate change, tectonism and volcanism. Sedimentology 61 (2), 383–410. doi:10.1111/sed.12066

Figure captions

Fig. 1. A) Simplified regional geological map indicating the main geological units in Chile and Argentina between 32°30’ S and 33°45’ S (based on Giambiagi and Ramos, 2003; Fock Kunstmann 2005; Muñoz et al., 2006; Charrier et al., 2014; Giambiagi et al., 2014; Porras et al., 2016). AFTB : Aconcagua Fold and Thrust Belt. B) Map of the Caheuta Basin infill in the study area, showing the outcrop extent of the Divisadero Largo, the Mariño and the La Pilona formations, overlying Neogene to Quaternary formations, and the approximate position and stratigraphic range of main logged sections (based on Irigoyen et al., 2000 and Giambiagi et al., 2015).

Fig. 2. Composite, schematic stratigraphic column through the Mariño and La Pilona formations (position of sampled beds are shown as hollow diamonds, vf: very fine-grained sandstones, m: medium-grained sandstones, v.c: very coarse-grained sandstones). The age at the bottom of the succession is an estimate based on data from Cerdeño and Vucetich (2007) and Buelow et al. (2014). Ages in bold are based on the magnetostratigraphic study of Irigoyen et al. (2000). A) Muddy alluvium moderately pedogenized and isolated channel fills. B) Well-sorted cross-stratified sandstones representing aeolian deposition. C) Alternating coarse-clastic amalgamated channel-fills and mudstone dominated overbank deposits. D) Conglomeratic fluvial-channel fills.

Fig. 3. Mineralogy of sandstone samples (according to QEMSCAN® measurements) through the stratigraphic column (vf: very fine-grained sandstones, m: medium-grained sandstones, vc: very coarse-grained sandstones). The succession is divided into seven letter-coded units based on compositional and sedimentological changes. Main mineralogy is given in area %. Main heavy-minerals (Fe-Ti-oxides, pyroxenes and amphiboles) are given in area % of the total content of heavy-minerals.

Fig. 4. Abundance of compatible and incompatible trace elements through stratigraphy (values are given in parts per million, ppm).

Fig. 5. K_2O/Na_2O vs. SiO_2 diagram of Roser and Korsch (1986) for the tectonic setting discrimination of sandstones from the Mariño and the La Pilona formations.

Fig. 6. Th-Sc-Zr/10 ternary diagram (Bhatia and Crook, 1986) for compositional discrimination of tectonic setting. The scaling factor has been used to bring the fields into the middle of the diagram without altering their relative position. OIA: oceanic island arc, ACM: active continental margin, CIA: continental island arc, PM: passive margin.

Fig. 7. Bivariant plot of SiO_2 vs. Al_2O_3+K_2O+Na_2O (Suttner and Dutta, 1986) expressing the chemical maturity of the sandstones as a function of climate.

Fig. 8. Log(Na_2O/K_2O) vs. log(SiO_2/Al_2O_3) diagram (Pettijohn et al., 1972; modified according to Herron et al., 1988) for the geochemical classification of terrigenous sands.

Fig. 9. Mineralogical and compositional variations of sandstones from the Mariño and La Pilona formations. The MIA is illustrated in the Qtz-Plg-Kfs (Quartz – Plagioclase - K-feldspar) mineralogical space and the CIA is illustrated in the A-CN-K (Al_2O_3-CaO*+Na_2O-K_2O) compositional space (based on Nesbitt and Young, 1986; Rieu et al., 2007; Roy and Roser, 2012 and Zhang et al., 2013). The data are deviated from the ideal weathering trend (IWT) probably due to a progressive change in the source-rock composition. The Plg-Kfs (plagioclase - K-feldspar) line can be used to infer the composition of the original bedrock source. Ba: basalt; An: andesite; Di: diorite; Da: dacite; G: granite; Rh: rhyolite (see text for further discussion).

Fig. 10. CIA and MIA representing, respectively, the chemical and mineralogical maturity of sandstones (vf: very fine-grained sandstones, m: medium-grained sandstones, vc: very coarse-grained sandstones). Clay-mineral content given in area % (sum of kaolinite, illite and smectite content in the samples according to QEMSCAN® measurements). The CIA trend of sandstones from the La Pilona Formation follows closely that of clay-mineral content, suggesting the effect of depositional concentration of clays on the weathering index. Th/Sc, Zr/Sc ratios and isotopic ratios of strontium and neodymium (epsilon notation) provide information on the character of igneous bedrock sources.

Fig. 11. Principal component analysis (PCA). The length of each ray is proportional to its variability among the data set. If the angle between two variables is close to 0°, 90° or 180°, then the

corresponding variables are directly correlated, uncorrelated or inversely correlated, respectively (Garzanti and Resentini, 2016). A) PCA based on the mineralogical composition of the sandstones from the Mariño and the La Pilona formations. First and second dimensions (PC1 and PC2) show the importance of the weathering signal and the concentration of clay- and heavy-minerals, respectively. The dashed arrow indicates the general weathering trend through stratigraphy. B) PCA carried out on major elements.

Fig. 12. Th/Sc vs. Zr/Sc plot (Roser and Korsch, 1999). The arrow indicates the trend expected from zircon (and other heavy-minerals) concentration by recycling processes. The dashed line shows the compositional trend from basalt to granite, proposed by Mongelli et al. (2006).

Fig. 13. K_2O+Na_2O vs. SiO_2 (TAS) classification diagram for the volcanic rocks (Le Maitre et al., 1989; modified after Alarcon and Pinto, 2015). Samples plot in the sub-alkaline field, but the composition might have been partly altered by the changing Na_2O concentration due to weathering. The compositional fields for the potential source rocks are given by Ramos et al. (1996b), Vergara and Nyström (1996), Llambías et al. (2003), Kay et al. (2005), Muñoz et al. (2006), Kleiman and Japas (2009).

Fig. 14. Zr/TiO_2 vs Nb/Y diagram (Winchester and Floyd, 1977) for source-rock recognition based on the composition of sedimentary rocks (Fralick 2003; Pinto et al., 2004). The compositional fields for the potential source rocks are given by Vergara and Nyström (1996), Llambías et al. (2003), Muñoz et al. (2006) and Kleiman and Japas (2009).

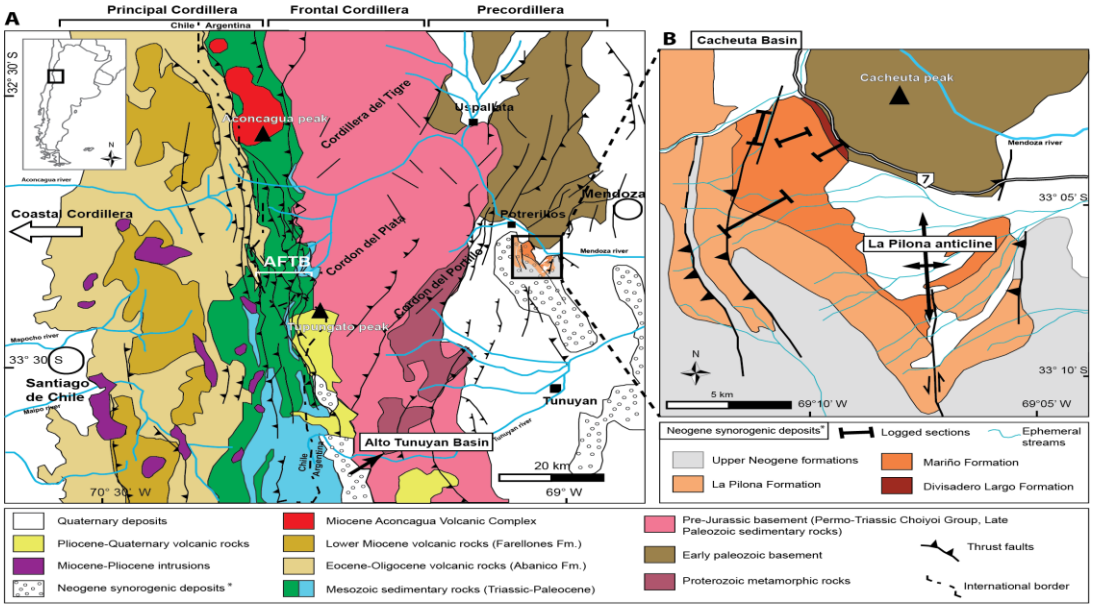

Figure 1

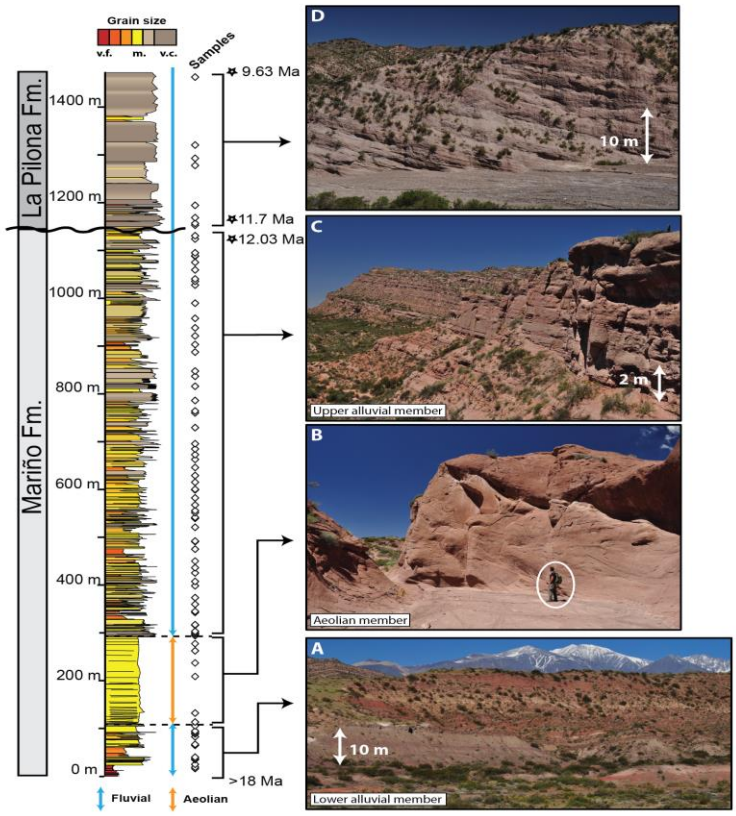

Figure 2

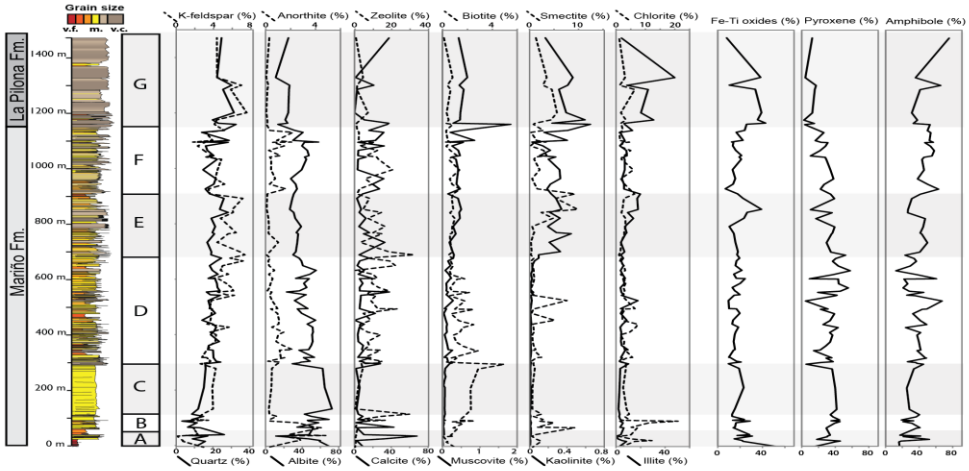

Figure 3

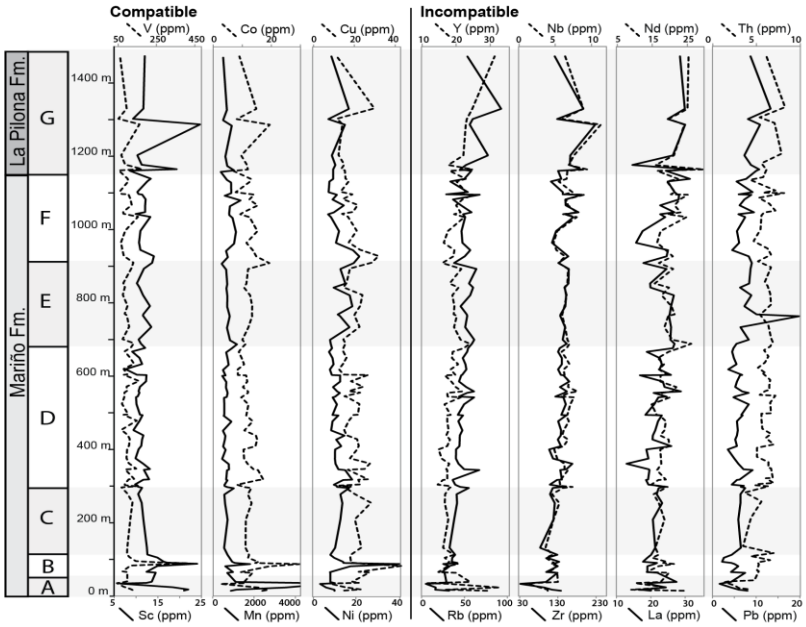

Figure 4

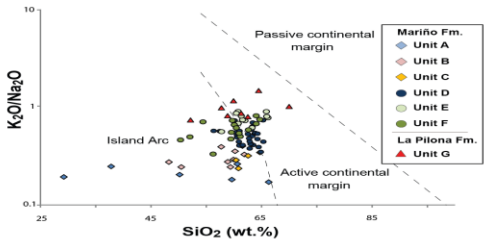

Figure 5

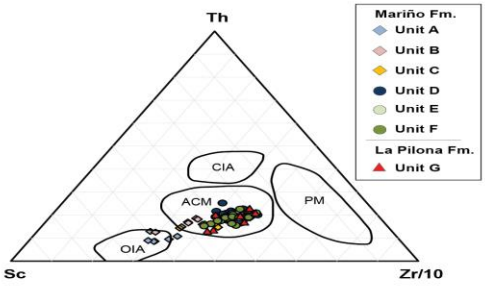

Figure 6

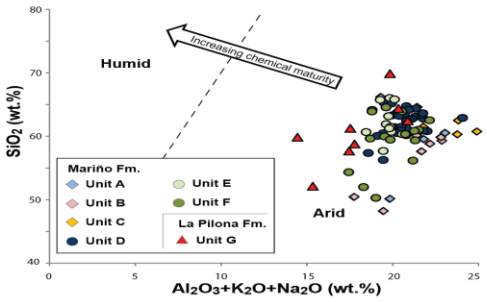

Figure 7

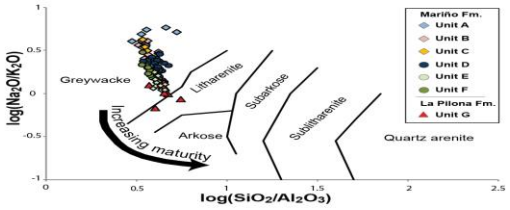

Figure 8

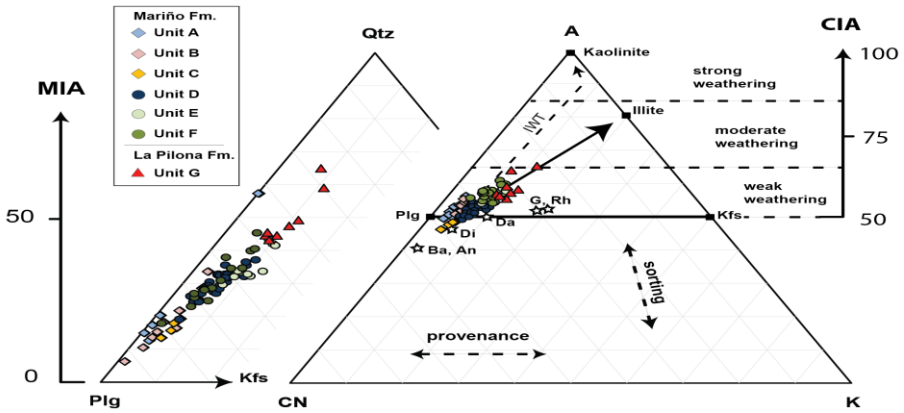

Figure 9

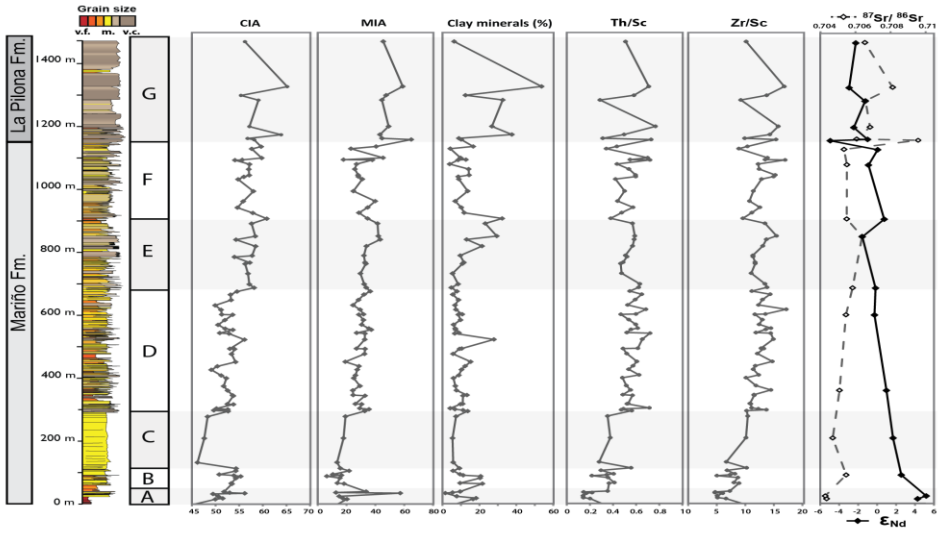

Figure 10

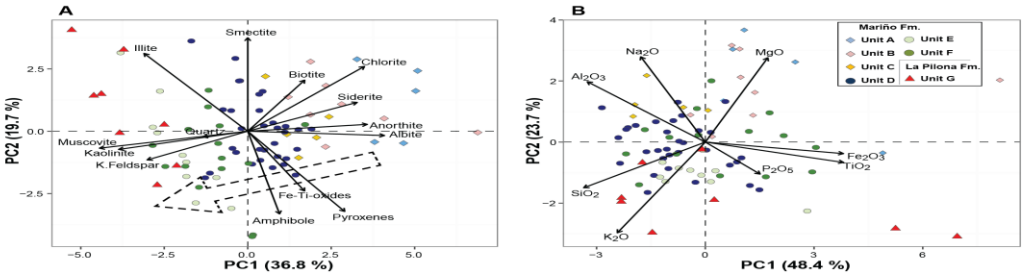

Figure 11

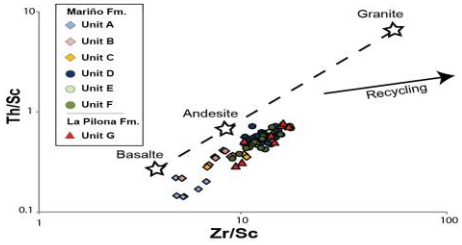

Figure 12

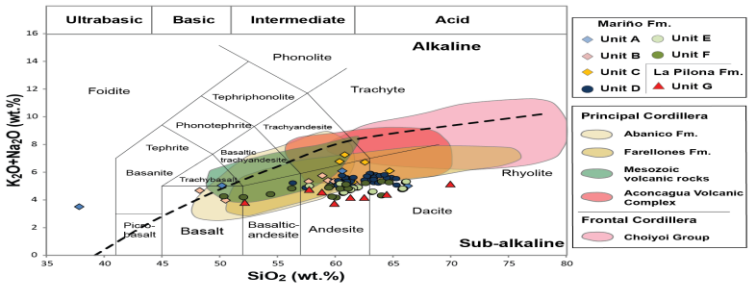

Figure 13

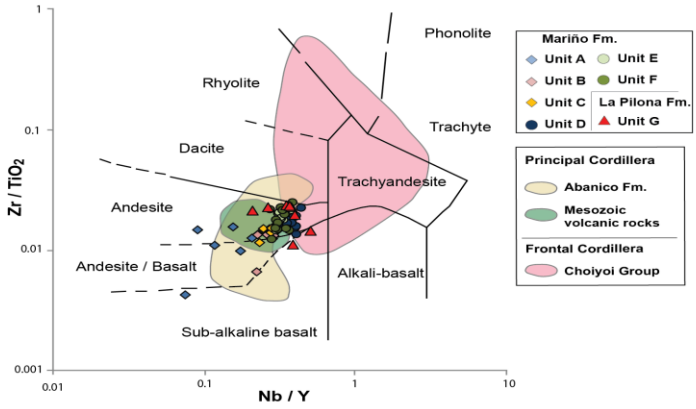

Figure 14